LA-3527

c . 3

LOS ALAMOS SCIENTIFIC LABORATORY
of the
University of California
LOS ALAMOS • NEW MEXICO

Neutron Cross Sections for ^{235}U and ^{238}U in the Energy Range 1 keV to 14 MeV

UNITED STATES
ATOMIC ENERGY COMMISSION
CONTRACT W-7405-ENG. 36

This report expresses the opinions of the author or authors and does not necessarily reflect the opinions or views of the Los Alamos Scientific Laboratory.

Printed in the United States of America. Available from
Clearinghouse for Federal Scientific and Technical Information
National Bureau of Standards, U. S. Department of Commerce
Springfield, Virginia 22151
Price: Printed Copy $3.00; Microfiche $0.65

LA-3527
UC-34, PHYSICS
TID-4500

LOS ALAMOS SCIENTIFIC LABORATORY
of the
University of California
LOS ALAMOS • NEW MEXICO

Report written: August 1968
Report distributed: September 5, 1968

Neutron Cross Sections for ^{235}U and ^{238}U in the Energy Range 1 keV to 14 MeV

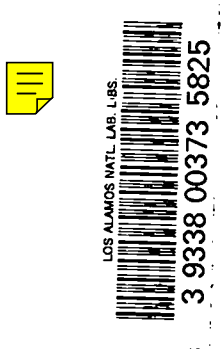

by

J.-J. H. Berlijn*
R. E. Hunter**
C. C. Cremer

*Present address: Physics Department, Valdosta State College, Valdosta, Georgia.

**Work begun while a LASL Staff Member, completed while in capacity of Consultant. Present address: Physics Department, Valdosta State College, Valdosta, Georgia.

NEUTRON CROSS SECTIONS FOR ^{235}U AND ^{238}U IN THE ENERGY RANGE 1 keV TO 14 MeV

by

J.-J. H. Berlijn, C. C. Cremer, and R. E. Hunter

ABSTRACT

Recommended cross sections for ^{235}U and ^{238}U are presented. Comparisons of calculated and experimental values of integral systems were used as a guide in choosing the fits to microscopic cross-section data.

I. INTRODUCTION

This report presents the results of a compilation of the available experimental data on the neutron-induced reaction cross sections for uranium isotopes, with the objective of providing consistent sets of cross sections for neutronics calculations in fast critical and supercritical systems. Because of the neutron flux spectra in these very fast systems, cross sections at incident neutron energies of 1 keV and lower are relatively unimportant. Cross sections are presented from 1 keV to 14 MeV.

Extensive comparisons were made with a host of integral experiments, such as bare and reflected critical assemblies, spectral indices, and central core reactivity contributions.[1] Each of these comparisons provided a further check on the experimental data, and in some cases led to alteration of the previously chosen best fit to the data.

Several compilations of experimental and theoretical neutron cross sections already exist whose authors have recommended "best fits" to the data presented. The experimental uncertainty of these data is usually about 5% or greater, and variations in these fits may justifiably be made within this uncertainty. However, there exist many integral experiments such that certain choices of these fits to the data lead to calculations of the integral quantity which lie outside the range of experimental error.

A good example is the critical mass of 93.5% enriched uranium which was measured in the Lady Godiva assembly. The critical mass is known to within ± 0.1%. However, the uncertainty of ± 5% in the fission cross section of ^{235}U leads to a calculational uncertainty of ± 12% in the critical mass. It is believed that the calculational techniques available on modern computers are capable of calculating the critical mass of this assembly to ± 0.2%. Integral experiments such as this may therefore be thought of as placing one more constraint upon the "best fit" to the microscopic cross-section data.

The purpose of this report is to present such a set of recommended data which has been tested over a range of integral experiments and which has been found to give agreement within experimental error for all such integral quantities that have been calculated. It is not intended that these curves should be considered as being

a refinement on the experimental data, or "better" in some nebulous sense than the experimental data, nor do the authors contend that the experimental uncertainty in the data has been somehow reduced. All that is claimed is that these recommended curves represent a particular set of fits to the experimental data which is consistent with the integral experiments.

It is recognized, of course, that this recommended set of curves is not unique. However, it is felt that it represents a useful step in the processing of neutron cross-section data for use in neutronics calculations. Indeed, the cross-section user may often find that to achieve the accuracy required of his calculations a normalization of this type is essential. Needless to say, the final element of responsibility for checking one's calculations against those experiments which bear most directly on the problem under study must still fall on the user.

In this respect it should be noted that the sensitivity of the calculations of integral experiments to variations in the cross sections within an energy range is proportional to the total flux within that energy range. Since all integral experiments used in the above tests were performed on fast assemblies, confidence in the recommended curves is highest in the range 0.1 to 6 MeV, and drops at both the low and high ends of the energy range.

This report is not intended to represent a comprehensive compilation of experimental data, with best fits to these data alone. Rather, the best fits were used as initial input to calculations for comparison with the series of integral experiments as described above. These results were then used to modify the initial best fits in such a way that consistent results were obtained for all calculations. Attempts were made to keep these modifications within the experimental errors on the data. In fact, for the cross sections presented in this report, these modifications were approximately 3% or less, except where noted.

The calculational techniques used in computing the integral experiments were carried to the point where numerical and calculational approximations introduce errors which are comparable to, or less than, the experimental errors on the integral quantities.

These calculations and comparison with the integral experimental results are described in detail in the authors' report LA-3529.[1]

II. CALCULATIONAL PROCEDURE

The energy region of interest extends from 1 keV to 14 MeV. Over this region the cross sections of importance are:

total cross section	$\sigma_{n,T}$
fission cross section	$\sigma_{n,F}$
elastic scattering cross section	$\sigma_{n,n}$
inelastic scattering cross section	$\sigma_{n,n'}$
radiative capture cross section	$\sigma_{n,\gamma}$
n,2n cross section	$\sigma_{n,2n}$
n,3n cross section	$\sigma_{n,3n}$

To accurately represent the final-state neutron spectra, it is desirable to represent the fission cross section as the sum of three cross sections:

$$\sigma_{n,F} \quad \sigma_{n,f} + \sigma_{n,n'f} + \sigma_{n,2nf}.$$

$\sigma_{n,f}$ will denote the direct fission cross section, with $\sigma_{n,F}$ the total fission cross section.

The cross-section data, along with neutron energy and angular distributions, were processed by a digital computer program which calculated a flux-weighted average of each cross section over a specified set of energy groups. These group cross sections were then employed in a calculation using the Carlson discrete S_n approximation to the Boltzmann transport equation to test the cross sections with integral experiments. The microscopic data were then

adjusted where necessary to give agreement with the integral experiments. For details of the calculational techniques, the reader is referred to LA-3529.

III. URANIUM-235

For the well-established cross sections, no attempt has been made to catalog every report on the subject; rather a reference is given to an already existing compilation. Individual reports are referenced if they are not included in such a compilation.

A. Total Cross Section

The total cross section for ^{235}U was essentially based on the compilations of Hughes and Schwartz,[2] Stehn et al.,[3] and Parker.[4] Between 1 and 10 keV the data given in Stehn et al. are not plotted because of the great number of points and the apparent structure of the cross section. The recommended curve in that energy region follows an average of those points.

B. Elastic Scattering Cross Section

The elastic scattering cross section was based on the compilation of Stehn et al., as well as the best fit curves given by Schmidt[5] and by Parker. In addition, the data of Smith[6] between 30 keV and 1.5 MeV were used.

C. Fission Cross Section

The total fission cross section was taken from Hughes and Schwartz, Stehn et al., Parker, and White.[7] The threshold for $\sigma_{n,n'f}$ was taken to be 6 MeV. Above this energy, the direct fission cross section, $\sigma_{n,f}$, was taken to be a constant. The threshold for $\sigma_{n,2nf}$ was taken to be 11.5 MeV, with $\sigma_{n,n'f}$ assumed to be constant above this energy. From the total fission cross-section curve in Fig. 3 (at the end of this report), one can see that these thresholds correspond to sharp increases in the total fission cross section, and that immediately below these thresholds $\sigma_{n,F}$ is tending toward a constant value.

D. n,2n and n,3n Cross Sections

$\sigma_{n,2n}$ and $\sigma_{n,3n}$ were taken from Parker and Schmidt. The curves from these reports were used to construct smoothly varying curves which generally follow the recommendations of the two authors. The energy distribution for these processes is described in Sec. III-H.

E. Radiative Capture Cross Section

The radiative capture cross section was computed, using the experimental data for the fission cross section and the capture-to-fission ratio, α, as given in the compilations of Parker, Hughes and Schwartz, Stehn et al., and Schmidt. In order to obtain better agreement with reflected critical assemblies, the capture cross section was chosen high with respect to the mean of the experimental data. However, these measurements have a quoted uncertainty of 15 to 20%, and the recommended curve lies well within this range.

F. Inelastic Scattering Cross Section

We can write

$$\sigma_{n,T} = \sigma_{n,F} + \sigma_{n,n} + \sigma_{n,\gamma} + \sigma_{n,n'} + \sigma_{n,2n} + \sigma_{n,3n'} \quad (1)$$

so that

$$\sigma_{n,n'} = \sigma_{n,T} - \sigma_{n,F} - \sigma_{n,n} - \sigma_{n,\gamma} - \sigma_{n,2n} - \sigma_{n,3n}. \quad (2)$$

Equation 2 was used to establish the general behavior of the total inelastic scattering

The inelastic scattering cross section is, in reality, a sum of cross sections for excitation of residual nuclear levels. These partial cross sections, as they will be called, have characteristic shapes. The energy levels of ^{235}U were obtained from Baranov et al.[8] and Horsch.[9] The partial cross sections were then constructed in such a manner that their sum was consistent with $\sigma_{n,n'}$ as determined from Eq. 2.

The final-state neutron energy spectrum, was measured by Cranberg at 0.55, 0.98, and 2 MeV.[10] The measurements at 0.98 and 2 MeV are in good agreement with statistical theory. Rather than specify the partial cross sections for the very numerous levels above 200 keV, these levels were combined to give the partial cross section for the "statistical model." (See Section III-G.)

G. Neutron Energy Distributions for Evaporation Processes

As stated above, the energy distribution of secondary neutron from inelastic scattering at 980 keV was in good agreement with statistical theory. The resulting energy spectrum may be fit well by an evaporation formula of the form:

$$F(E) = \frac{E}{T^2} e^{-E/T} \qquad (3)$$

where T characterizes the nuclear temperature.

The spectra measured by Cranberg at 0.98 and 2.0 MeV can be fit with temperatures of 0.35 and 0.4 MeV, respectively. At 14.3 MeV, Vasilev et al.[11] have measured the spectrum of all secondary neutrons following a fission event. These include evaporation neutrons from (n,n'f) and (n,2nf) reactions. The spectrum was fit with Eq. 3 to represent prefission evaporation neutrons, plus a fission spectrum representation. The temperature for the evaporation component was found to be 0.37 ± 0.04 MeV.

Zamyatnin et al.[12] performed a similar experiment for 14-MeV neutrons in which the spectrum of all secondary neutrons was measured. The evaporation component of the spectrum included (n,n'), (n,2n), and (n,3n) neutrons in addition to prefission evaporation neutrons. The temperature which best fit the spectrum for all evaporation neutrons was found to be 0.4 ± 0.05 MeV.

It appears that the energy distribution for all evaporation neutrons can be adequately fit with a temperature of 0.4 MeV for incident neutron energies between 2 and 14 MeV. Although the temperature for separate processes, such as (n,n') and (n,2nf), may differ in detail, when all evaporation processes are combined a constant temperature above 2 MeV seems to be adequate. With respect to neutronics calculations, the only requirement is that the overall spectrum be correct. We have therefore assigned one temperature to all evaporation neutrons.

The n,n' spectrum measured by Cranberg at 550 keV is not well fit by an evaporation calculation alone. The best fit appears to result from a combination of an evaporation spectrum plus discrete lines from scattering from low lying levels.

If the excitation energy of nuclide A is given by E_i^*, and the energy of the incident neutron in the lab system is given by E, then, on the average, the final neutron energy after an inelastic collision is given by

$$\left\{E_{final}\right\}_i = \frac{1 + A^2\left[1-\left(\frac{A+1}{A}\right)\frac{E_i^*}{E}\right]}{(1 + A)^2} E. \qquad (4)$$

The spectrum at 550 keV was fit with an evaporation spectrum with T = 0.25 MeV, plus contributions due to discrete levels below 200 keV, with the final state energy for discrete levels calculated from Eq. 4. The curves of partial cross sections shown in Fig. 6 reflect the weight given to the evaporation spectrum. The curves for the discrete levels deviate (at energies above about 500 keV) from the measured excitation curves; an increasing fraction of the excitation curves at higher energies is contained in the "statistical model" cross section. Again, the only requirement for neutronics calculations is that the overall spectrum be correct, and this is achieved by the above procedure, with the choice of temperatures as follows:

E (MeV)	T (MeV)
0.20	0.20
0.55	0.25
0.98	0.35
2.0	0.4
14	0.4

H. Number of Neutrons per Fission

The curve of the mean number of final-state neutrons per fission, $\bar{\nu}$, was obtained from the data of Mather et al.,[13] Diven and Hopkins,[14] Meadows and Whalen,[15] Sowerby,[16] and Moat et al.,[17] along with the compilation of Stehn et al. These data can be fit to a linear term in energy over three sections of the energy region as follows:

$$\bar{\nu} = 2.420 + 0.112\ E\ (\text{MeV}), \quad 0 \leq E \leq 3.0\ \text{MeV}$$

$$\bar{\nu} = 2.199 + 0.185\ E\ (\text{MeV}), \quad 3.0 \leq E \leq 8.0\ \text{MeV}$$

$$\bar{\nu} = 2.898 + 0.98\ E\ (\text{MeV}), \quad 8.0 \leq E \leq 14\ \text{MeV}$$

I. Fission Neutron Energy Distribution

The values of $\bar{\nu}$ in the above section include all fission neutrons. However, we have separated the total fission cross section into three quantities:

$$\sigma_{n,F} = \sigma_{n,f} + \sigma_{n,n'f} + \sigma_{n,2nf}.$$

One neutron from $\sigma_{n,n'f}$ and two neutrons from $\sigma_{n,2nf}$ are treated as evaporation neutrons, in the sense of the statistical model described above. The fission neutrons are then regarded as

$$\bar{\nu}\,\sigma_{n,f} + (\bar{\nu}-1)\,\sigma_{n,n'f} + (\bar{\nu}-2)\sigma_{n,2nf}$$

and are distributed according to the final-state prompt fission neutron energy spectrum. This spectrum was measured by Vasilev et al.,[11] Zamyatnin et al.,[12] Cranberg et al.,[18] Grundl and Usner,[19] Grundl,[20] and Skarsvåg and Bergheim.[21] The spectrum has been fitted by a Maxwellian distribution:

$$\theta(E) = \frac{2}{\sqrt{\pi}}\ \frac{1}{T^{3/2}}\ E^{1/2}\ e^{-E/T} \qquad (5)$$

and by the well known sinh law:

$$\theta(E) = \frac{1}{\sqrt{\pi\,\omega\,T_f}}\ e^{-\omega/T_f}\ e^{-E/T_f} \sinh \frac{(2\,\omega\,E)}{T_f} \qquad (6)$$

where T_f and ω are parameters. The errors are generally such as to preclude a clear choice between Eqs. 5 and 6. For consistency, the authors have used Eq. 5 to fit all experimental distributions.

The best fits to the data of Cranberg et al. and Grundl are obtained for T = 1.29 MeV (for incident neutrons of thermal energy). Barnard et al.[22] give 1.297 MeV at thermal energy, and provide a good compilation of other experimental values for this quantity for various isotopes at different incident energies. The data of Vasilev et al.[11] at 14.3 MeV and that of Zamyatnin et al.[12] at 14.0 MeV can be fit with Eq. 5 for T = 1.39 MeV and T = 1.38 MeV, respectively.

It was assumed that T(E) is a smoothly varying function of E. A theoretical expression for T(E) is given by Terrell,[23] who obtained a function relating the nuclear temperature to $\bar{\nu}$:

$$T(E) = A + B\left[\bar{\nu}(E) + 1\right]^{1/2}. \qquad (7)$$

From the functional relation in Eq. 7, with T (thermal) = 1.29 and T (14 MeV) = 1.39, a curve of T versus E was obtained. With this curve to specify T as a function of the incident neutron energy, the final-state fission spectrum neutrons were distributed according to Eq. 5.

The prefission (evaporation) neutrons from the (n,n'f) and (n,2nf) processes were distributed in energy according to the statistical model, which is described in Sec. III-H.

For ^{235}U, Vasilev et al. measured the ratio of the prefission evaporation neutrons to all fission neutrons and obtained the value 0.16 ± 0.02. This compares with 0.18 obtained with the assignments of $\bar{\nu}$, $\sigma_{n,f}$, $\sigma_{n,n'f}$, and $\sigma_{n,2nf}$ as given above. Zamyatnin et al. measured the ratio of fission spectrum neutrons to all secondary neutrons, excluding

elastic scattering, and obtained 0.68 ± 0.06 for this ratio. This compares with 0.76 obtained from the recommended curves given in this report.

J. Delayed Neutrons

The delayed neutrons from ^{235}U have been measured by Bonner et al.[24] and by Batchelor and Hyder.[25] From their measurements, a curve of the relative number of delayed neutrons as a function of energy was constructed and is given in Fig. 10. The total delayed neutron fraction is given by Keepin[26] to be 0.0064. This fraction was distributed as a function of energy according to the curve in Fig. 10.

K. Angular Distributions

The experimentally measured differential elastic scattering cross sections were fit with the expression

$$\frac{d\sigma_{n,n}}{d\Omega} = \frac{\sigma_{n,n}}{4\pi}\left[1 + \sum_{i}^{10} W_i P_i(\mu)\right], \quad (8)$$

where $P_i(\mu)$ are the Legendre polynomials, and $\mu = \cos\theta$. Smith[6] gives $W_1 - W_5$ between 300 keV and 1.5 MeV. These values were supplemented with the W_i from angular distributions at 0.5, 1.0, and 2.0 MeV obtained from Goldberg et al.[27] Above 2.0 MeV, the values for W_i for ^{235}U were extrapolated to intercept smoothly the corresponding curves for ^{238}U, which are described in Sec. IV-K. In order to calculate reflected critical assemblies it was necessary to slightly lower the W_1 curve with respect to the experimental data. For further details see LA-3529.

Nonelastic reactions were assumed to have isotropic angular distributions.

L. Recommended Curves

The cross-section curves for ^{235}U, along with the Legendre coefficients for $d\sigma_{n,n}/d\Omega$, are shown in Figs. 1 through 10. The experimental data from the above references are also plotted on these graphs. No attempt is made to identify the sources of the individual points. The cross sections are tabulated in Table I.

IV. URANIUM-238

The bare critical assembly used in comparison of the uranium cross sections contained only 5.25% of ^{238}U, giving a rather insensitive check of these cross sections. Thus the primary integral comparisons were made with spectral indices, central replacement measurements, and critical assemblies of natural-uranium-reflected plutonium and enriched uranium.

A. Total Cross Section

For the total cross section, the data given in the compilation of Parker[28] are used.

B. Radiative Capture Cross Section

The data of Hughes and Schwartz, Stehn et al., Parker,[28] and Barry et al.[29] were used for $\sigma_{n,\gamma}$.

The radiative capture cross section is given in Fig. 12. The solid curve gives the best fit to the data, with the more recent data being weighted more heavily than the other points. Various integral experiments were compared with the results as calculated by the authors.[1] These revealed serious discrepancies with $\sigma_{n,\gamma}$ which include spectral indices, criticality measurements on reflected assemblies, and core reactivity contributions, among others. Hansen[30] has indicated a similar difficulty in calculating these integral quantities with the experimental data as given above.

The dotted curve in Fig. 12 was constructed in an effort to obtain better agreement with these integral measurements. Agreement with the integral experiments was greatly improved by lowering the capture cross section as indicated. An alternative curve, also in agreement with the integral experiments, is given by the dashed line in Fig. 12, indicating the freedom allowed within the bounds of the integral experiments. An infinite set of curves can be drawn, using properly chosen combinations of the dashed curve and the dotted curve, all of which will essentially give agreement with the integral measurements.

Table I

TABULATED CROSS SECTIONS FOR ^{235}U IN BARNS

Energy (MeV)	$\sigma_{n,F}$	$\sigma_{n,n}$	$\sigma_{n,\gamma}$	$\sigma_{n,n'}$	$\sigma_{n,2n}$	$\sigma_{n,3n}$
0.0010	7.0	13.50	3.50	-	-	-
0.0015	6.20	14.07	2.75	-	-	-
0.0020	5.58	14.19	2.36	-	-	-
0.0025	5.22	14.01	2.11	-	-	-
0.0030	4.97	13.81	1.91	-	-	-
0.0040	4.38	13.39	1.64	-	-	-
0.0050	3.93	12.96	1.49	-	-	-
0.0060	3.63	12.66	1.38	-	-	-
0.0070	3.42	12.26	1.30	-	-	-
0.0080	3.28	11.84	1.23	-	-	-
0.0090	3.12	11.57	1.18	-	-	-
0.010	3.01	11.24	1.14	-	-	-
0.015	2.63	11.40	1.01	-	-	-
0.020	2.46	11.54	0.95	-	-	-
0.025	2.33	11.30	0.90	-	-	-
0.030	2.23	11.08	0.86	0.035	-	-
0.040	2.10	10.74	0.79	0.093	-	-
0.050	1.98	10.35	0.75	0.109	-	-
0.060	1.88	10.10	0.68	0.190	-	-
0.070	1.80	9.75	0.63	0.273	-	-
0.080	1.74	9.60	0.592	0.350	-	-
0.090	1.69	9.45	0.553	0.398	-	-
0.10	1.64	9.35	0.521	0.440	-	-
0.15	1.50	8.55	0.417	0.588	-	-
0.20	1.40	7.95	0.347	0.625	-	-
0.25	1.33	7.40	0.300	0.650	-	-
0.30	1.28	6.90	0.261	0.665	-	-
0.40	1.19	6.20	0.206	0.690	-	-
0.50	1.14	5.55	0.193	0.740	-	-
0.60	1.13	5.00	0.183	0.83	-	-
0.70	1.13	4.70	0.171	0.91	-	-
0.80	1.14	4.52	0.154	1.00	-	-
0.90	1.15	4.30	0.139	1.08	-	-
1.0	1.17	4.07	0.121	1.17	-	-
1.5	1.21	4.01	0.065	1.38	-	-
2.0	1.28	4.23	0.042	1.51	-	-
2.5	1.25	4.55	0.030	1.63	-	-
3.0	1.18	4.85	0.023	1.69	-	-
3.5	1.10	4.87	0.018	1.72	-	-
4.0	1.05	4.82	0.015	1.76	-	-
4.5	1.05	4.62	0.012	1.78	-	-
5.0	1.05	4.37	0.010	1.80	-	-
5.5	1.06	4.14	-	1.79	0.015	-
6.0	1.08	3.99	-	1.70	0.090	-
6.5	1.35	3.85	-	1.27	0.302	-
7.0	1.59	3.65	-	0.90	0.450	-
7.5	1.69	3.49	-	0.73	0.488	-
8.0	1.77	3.35	-	0.63	0.526	-
8.5	1.81	3.14	-	0.545	0.566	-
9.0	1.83	3.09	-	0.480	0.600	-
9.5	1.82	3.00	-	0.437	0.632	-
10.0	1.81	2.96	-	0.412	0.660	-
10.5	1.80	2.92	-	0.398	0.690	-
11.0	1.80	2.89	-	0.389	0.697	-
11.5	1.80	2.92	-	0.380	0.670	-
12.0	1.81	2.97	-	0.372	0.600	-
12.5	1.86	3.03	-	0.361	0.510	0.008
13.0	1.95	3.08	-	0.349	0.410	0.020
13.5	2.07	3.12	-	0.338	0.270	0.040
14.0	2.18	3.16	-	0.328	0.130	0.060

However, it should be noted that none of these curves can be drawn so as to remain within the experimental errors on the cross-section data at all energies. Thus, there is an unresolved discrepancy between the integral measurements and the experimental cross-section data.

This subject is discussed in some detail in Ref. 1, which presents the results of several comparisons. In the absence of any experimental indication of the source of this discrepancy, the dotted curve in Fig. 12 is recommended for calculations of fast assemblies. This is admittedly a somewhat arbitrary choice from the family of curves described above, and does not constitute a claim on the part of the authors that the rise in $\sigma_{n,\gamma}$ around 1 MeV does not exist.

C. Inelastic Scattering Cross Section

A technique similar to the one described in Sec. III-F was used in constructing the inelastic scattering cross section. Energy levels were taken from the data given by Stehn et al.,[3] Parker,[28] and Smith,[31] who gave values for the partial cross sections. The partial cross-section curves as given in this report were chosen such that a smoothly varying total inelastic cross section as a function of energy was obtained.

Total inelastic cross-section measurements were also given by Batchelor et al.[32] and by Hanna and Clarke.[33]

Above 1.2 MeV, the inelastic scattering cross section was described by the statistical model.

D. Neutron Energy Distributions for Evaporation Processes

As was discussed in Sec. III-G, the energy distribution of neutrons from all evaporation processes can be described by Eq. 3 with a single temperature for all reactions. Values of the nuclear temperature were obtained from Vasilev et al.,[11] Zamyatnin et al.,[12] Parker,[28] Batchelor et al.,[32] and Hanna and Clarke. All levels above 930 keV were included in the statistical model cross section, which is used to describe the entire spectrum above 1.2 MeV. The values of T were chosen to be

E (MeV)	T (MeV)
1.0	0.26
4.0	0.45
7.0	0.54
14	0.55

E. Fission Cross Section

The fission cross section was taken essentially from the data of Stehn et al.,[3] Schmidt,[5] Parker,[28] and Hanna and Clarke.[33] Thresholds for $\sigma_{n,n'f}$ and $\sigma_{n,2n}$ are 5.3 and 12.83 MeV, respectively. Above the $\sigma_{n,n'f}$ threshold, $\sigma_{n,f}$ was taken to be a constant. Above the $\sigma_{n,2nf}$ threshold, both $\sigma_{n,f}$ and $\sigma_{n,n'f}$ were taken to be constant.

As a test of these assignments, the ratio of all evaporation secondary neutrons to the total number of secondary neutrons was calculated. This ratio was found to be 0.48, which compares to 0.49 ± 0.05 as measured by Zamyatnin et al.[12] The ratio of fission evaporation neutrons to all fission neutrons was found to be 0.15, as compared to the value of 0.21 ± 0.02 given by Vasilev et al.[11]

F. n,2n and n,3n Cross Sections

Values for the n,2n cross section were taken from Knight et al.[34] These data have recently been corrected, and the corrected data, obtained from Stewart,[35] are shown in Fig. 17. Data for $\sigma_{n,3n}$ are given by Stehn et al.[3] However, Stewart has further noted that these data are based to some extent on the incorrect values for $\sigma_{n,2n}$, and that a much lower n,3n cross-section curve must be drawn in order to obtain agreement with other parameters. The curve for $\sigma_{n,3n}$ in Fig. 17 is based on her calculations.

The final-state neutron energy distributions are described in Sec. IV-D.

G. Elastic Scattering Cross Section

Measurements of $\sigma_{n,n}$ between 300 and 1500 keV are given by Smith,[31] and at 2, 3, 4, and 7 MeV by Batchelor et al.[32] Values of $\sigma_{n,n}$ were also calculated from Eq. 2 since, in the case of ^{238}U, all other cross sections are more or less known. Calculations of $\sigma_{n,n}$ by Stewart[35] were also used in establishing the elastic scattering cross section above 3 MeV.

H. Number of Neutrons per Fission

The mean number of neutrons per fission is based on the data of Asplund-Nilsson et al.[36] supplemented by the data given by Parker[28] and Hanna and Clarke.[33] The data can be fit with a linear term in energy:

$$\bar{\nu} = 2.380 + 0.149\ E\ (\text{MeV}).$$

I. Fission Neutron Energy Distribution

Again the evaporation neutrons from $\sigma_{n,n'f}$ and $\sigma_{n,2nf}$ were described by the statistical model (Sec. IV-D). The prompt-fission neutron energy distribution is well described by Eq. 5, with the nuclear temperatures given by Vasilev et al.,[11] Zamyatnin et al.,[12] and Barnard et al.[22] Values of T were taken to be:

E (MeV)	T (MeV)
0.0	1.15
2.09	1.29
4.91	1.42
14.1	1.48

A smooth curve was drawn through these points, with the value at zero energy obtained by extrapolation. The final-state fission spectrum neutron energy distribution was then obtained from Eq. 5.

J. Delayed Neutrons

The delayed neutron fraction for ^{238}U is given by Keepin[26] and by Rose and Smith,[37] and was taken to be 0.0147. The energy distribution of these delayed neutrons was taken to be the same as for ^{235}U. The graph of relative number of neutrons as a function of energy is shown in Fig. 10.

K. Angular Distributions

The differential elastic scattering cross section was fit with Eq. 8. Smith[31] gives the values of W_1 - W_5 from 300 keV to 1.5 MeV. These results were supplemented by the W_i from angular distributions at 0.5, 1.0, 2.0, 2.5, 4.0, 7.0, and 14 MeV as given by Goldberg et al.[27] and by the measurements of Batchelor et al.[32]

Again, the inelastic scattering angular distribution was taken to be isotropic.

L. Recommended Curves

The cross-section curves for ^{238}U, along with the Legendre coefficients for $d\sigma_{n,n}/d\Omega$, are shown in Figs. 10 through 19. Experimental data from the references above are also plotted on these graphs. The cross sections are tabulated in Table II.

ACKNOWLEDGMENTS

The authors are very happy to acknowledge the help of C. P. Cadenhead and K. F. Famularo of LASL Group W-4 in providing many suggestions and critical evaluations of the results of this effort. B. C. Diven of LASL Group P-3 and Leona Stewart of P-DO were very helpful in evaluating microscopic cross sections. G. E. Hansen and J. A. Grundl of LASL Group N-2 provided many helpful comments related to bare assemblies and integral experiments, and their help was indispensible to the success of this effort. The cross-section compilation by K. Parker of Atomic Weapons Research Establishment, United Kingdom, provided a starting point for much of the work of this report and is gratefully acknowledged. Finally, the authors would like to thank N. C. Sanchez and B. A. Wellnitz of W-4 for their help in putting this report together and making it readable.

Table II

TABULATED CROSS SECTIONS FOR ^{238}U IN BARNS

Energy (MeV)	$\sigma_{n,F}$	$\sigma_{n,n}$	$\sigma_{n,\gamma}$	$\sigma_{n,n'}$	$\sigma_{n,2n}$	$\sigma_{n,3n}$
0.0010	-	13.35	1.74	-	-	-
0.0015	-	13.90	1.43	-	-	-
0.0020	-	14.03	1.24	-	-	-
0.0025	-	14.03	1.11	-	-	-
0.0030	-	14.03	1.01	-	-	-
0.0040	-	14.03	0.88	-	-	-
0.0050	-	14.08	0.795	-	-	-
0.0060	-	14.13	0.735	-	-	-
0.0070	-	14.11	0.695	-	-	-
0.0080	-	14.08	0.670	-	-	-
0.0090	-	14.06	0.660	-	-	-
0.010	-	14.05	0.649	-	-	-
0.015	-	13.90	0.580	-	-	-
0.020	-	13.65	0.508	-	-	-
0.025	-	13.30	0.451	-	-	-
0.030	-	13.10	0.415	-	-	-
0.040	-	12.78	0.346	-	-	-
0.050	-	12.32	0.302	0.043	-	-
0.060	-	12.09	0.269	0.116	-	-
0.070	-	11.93	0.243	0.203	-	-
0.080	-	11.57	0.226	0.278	-	-
0.090	-	11.16	0.210	0.345	-	-
0.10	-	11.04	0.198	0.405	-	-
0.15	-	10.02	0.162	0.685	-	-
0.20	-	9.31	0.143	0.888	-	-
0.25	-	8.69	0.132	1.05	-	-
0.30	-	8.19	0.122	1.18	-	-
0.40	-	7.27	0.111	1.39	-	-
0.50	-	6.71	0.107	1.54	-	-
0.60	-	6.15	0.102	1.62	-	-
0.70	-	5.58	0.099	1.70	-	-
0.80	-	5.06	0.096	1.84	-	-
0.90	-	4.72	0.094	1.91	-	-
1.0	0.015	4.41	0.092	2.02	-	-
1.5	0.0330	3.67	0.077	2.55	-	-
2.0	0.520	3.83	0.054	2.54	-	-
2.5	0.520	4.12	0.037	2.54	-	-
3.0	0.520	4.40	0.027	2.53	-	-
3.5	0.520	4.53	0.021	2.51	-	-
4.0	0.520	4.37	0.016	2.50	-	-
4.5	0.520	4.16	0.013	2.47	-	-
5.0	0.520	3.95	0.011	2.41	-	-
5.5	0.520	3.82	-	2.37	-	-
6.0	0.580	3.76	-	2.31	-	-
6.5	0.770	3.60	-	1.91	0.106	-
7.0	0.900	3.43	-	1.50	0.56	-
7.5	0.975	3.34	-	1.18	0.99	-
8.0	0.975	3.23	-	0.902	1.27	-
8.5	0.975	3.18	-	0.797	1.43	-
9.0	0.975	3.07	-	0.581	1.56	-
9.5	0.975	3.06	-	0.472	1.62	-
10.0	0.975	3.05	-	0.386	1.65	-
10.5	0.975	3.05	-	0.334	1.66	-
11.0	0.975	3.05	-	0.289	1.63	-
11.5	0.975	3.05	-	0.252	1.57	-
12.0	0.975	3.05	-	0.219	1.50	0.032
12.5	0.975	3.05	-	0.196	1.38	0.113
13.0	1.00	3.05	-	0.174	1.26	0.200
13.5	1.03	3.05	-	0.158	1.11	0.320
14.0	1.07	3.05	-	0.145	0.94	0.428

REFERENCES

1. C. C. Cremer, R. E. Hunter, and J.-J. H. Berlijn, "Comparison of Calculations with Integral Experiments for Plutonium and Uranium Critical Assemblies," LA-3529 (1968).
2. D. J. Hughes and R. B. Schwartz, "Neutron Cross Sections," BNL-325, 2nd Edition (1958).
3. J. R. Stehn, M. D. Goldberg, R. Wiener-Chasman, S. F. Mughabghab, B. A. Magurno and V. M. May, "Neutron Cross Sections," BNL-325, 2nd Edition, Supplement No. 2 (1965).
4. K. Parker, "Neutron Cross Sections of U^{235} and U^{238} in the Energy Range 1 keV - 15 MeV," AWRE-0-82/63 (1963).
5. J. J. Schmidt, "Neutron Cross Sections for Fast Reactor Materials," KFK-120 (1962).
6. A. B. Smith, "Elastic Scattering of Fast Neutrons from U^{235}," Nucl. Sci. Eng. 18, 126 (1964).
7. P. H. White, "Measurements of the U^{235} Neutron Fission Cross Sections in the Energy Range 0.04 MeV to 14 MeV," J. Nucl. Energy 19, 325 (1965).
8. S. A. Baranov, V. M. Kulakov, and S. H. Belenkii, "Fine Structure of Pu^{239} Alpha Radiation," Zh. Eksperim. i Teor. Fiz. 43, 1135 (1962); JETP 16, 801 (1963); Nucl. Phys. 41, 95 (1963).
9. F. Horsch, "Excited Energy Levels in U^{235}," Z. Physik 183, 352 (1965).
10. L. Cranberg, "Neutron Scattering by U^{235}, Pu^{239}, and U^{238}," LA-2177 (1959).
11. Yu. A. Vasilev, Yu. S. Zamyatnin, Yu. I. Ilin, E. I. Sirotinin, P. V. Toropov, and E. F. Fomushkin, "Measurements of the Spectra and Average Number of Neutrons Emitted in the Fission of U^{235} and U^{238} Induced by 14.3 MeV Neutrons," Zh. Eksperim. i Teor. Fiz. 38, 671 (1960); JETP 11, 483 (1960).
12. Yu. S. Zamyatnin, I. N. Safina, E. K. Gutnikova, and N. I. Ivanova, "Spectra of Neutrons Produced by 14-MeV Neutrons in Fissile Materials," At. Energ. (USSR) 4, 337 (1958); Soviet J. At. Energy 4, 443 (1958).
13. D. S. Mather, P. Fieldhouse, and A. Moat, "Average Number of Prompt Neutrons from U^{235} Fission Induced by Neutrons from Thermal to 8 MeV," Phys. Rev. 133, B1403 (1964).
14. B. Diven and J. Hopkins, private communication to Mather et al., Ref. 13, 1964.
15. J. W. Meadows and J. F. Whalen, "Energy Dependence of Prompt $\bar{\nu}$ for Neutron Induced Fission of U^{235}," Phys. Rev. 126, 197 (1962).
16. M. G. Sowerby, private communication (1964).
17. A. Moat, D. S. Mather, and M. H. Mactaggart, "Some Experimental Determinations of the Number of Prompt Neutrons from Fission," J. Nucl. Energy 15, 102 (1961).
18. L. Cranberg, G. Frye, N. Nereson, and L. Rosen, "Fission Neutron Spectrum of U^{235}," Phys. Rev. 103, 662 (1956).
19. J. Grundl and A. Usner, "Spectral Comparisons with High Energy Activation Detectors," Nucl. Sci. Eng. 8, 598 (1960).
20. J. Grundl, "Study of Fission Neutron Spectra with High-Energy Activation Detectors," LAMS-2883 (1963).
21. K. Skarsvåg and K. Bergheim, "Energy and Angular Distributions of Prompt Neutrons from Slow Neutron Fission of U^{235}," Nucl. Phys. 45, 72 (1963).

22. E. Barnard, A. T. G. Ferguson, W. R. McMurray, and I. J. VanHeerden, "Time-of-Flight Measurements of Neutron Spectra from the Fission of U^{235}, U^{238} and Pu^{239}," Nucl. Phys. 71, 228 (1965).

23. J. Terrell, "Fission Neutron Spectra and Nuclear Temperatures," Phys. Rev. 113, 527 (1959).

24. T. W. Bonner, S. J. Bame, Jr., and J. E. Evans, "Energy of the Delayed Neutrons from the Fission of U^{235}," Phys. Rev. 101, 1514 (1956).

25. R. Batchelor and H. R. M. Hyder, "The Energy of Delayed Neutrons from Fission," J. Nucl. Energy 3, 7 (1955).

26. G. R. Keepin, "Basic Kinetics Data and Neutron-Effectiveness Calculations," TID-7662, p. 334 (1964).

27. M. D. Goldberg, V. M. May, and J. S. Stehn, "Angular Distributions in Neutron-Induced Reactions, Vol. II," BNL-400, 2nd Edition (1962).

28. K. Parker, "Neutron Cross-Sections of U^{235} and U^{238} in the Energy Range 1 keV - 15 MeV," AWRE-0-79/63 (1963).

29. J. F. Barry, J. Bunce, and P. H. White, "Cross Section for the Reaction $U^{238}(n,\gamma)U^{239}$ in the Energy Range 0.12 - 7.6 MeV," J. Nucl. Energy 18, 481 (1964).

30. G. Hansen, private communication (1966).

31. A. B. Smith, "Scattering of Fast Neutrons from Natural Uranium," Nucl. Phys. 47, 633 (1963).

32. R. Batchelor, W. B. Gilboy, and J. H. Towle, "Neutron Interactions with U^{238} and Th^{232} in the Energy Region 1.6 MeV to 7 MeV," Nucl. Phys. 65, 236 (1965).

33. G. C. Hanna and R. L. Clarke, "Neutron Evaporation in the 14 MeV Neutron Fission of Uranium," Can. J. Phys. 39, 967 (1961).

34. J. D. Knight, R. K. Smith, R. A. Nobles, and B. Warren, "$U^{238}(n,2n)U^{237}$ Cross Section from 6 to 10 MeV," Bull. Am. Phys. Soc. Ser. II, 2, 198 (1957).

35. L. Stewart, private communication, 1968.

36. I. Asplund-Nilsson, H. Condé, and N. Starfelt, "Measurement of Prompt $\bar{\nu}$ in Fast Neutron Fission of U^{238} Induced by Neutrons from 1.5 to 15 MeV," FOA-4 (1964).

37. H. Rose and R. D. Smith, "Delayed Neutron Investigations with the ZEPHYR Fast Reactor: Part II - The Delayed Neutrons Arising from Fast Fission in U^{235}, U^{233}n U^{238}, Pu^{239}, and Th^{232}," J. Nucl. Energy 4, 133 (1957).

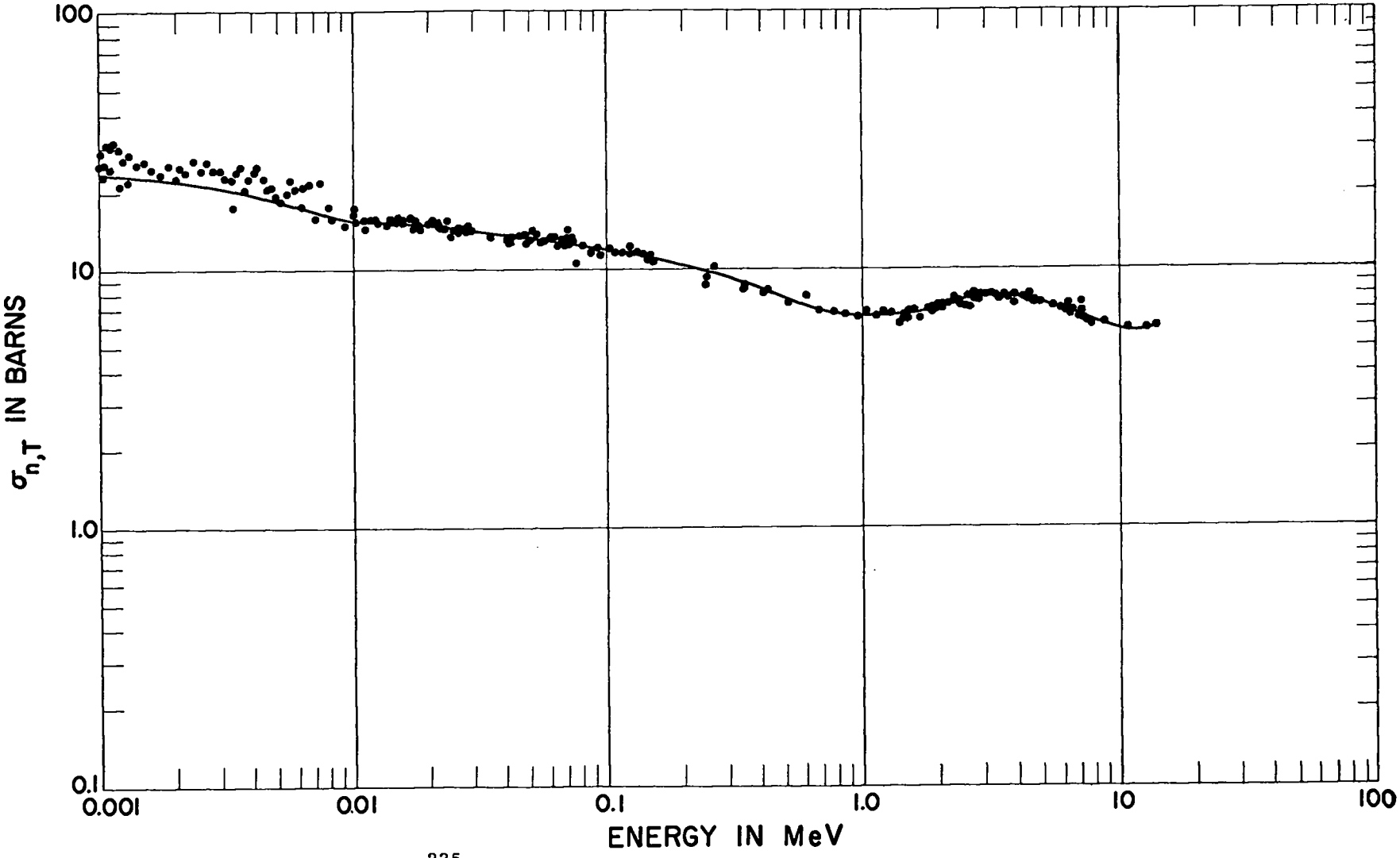

Fig. 1. Total cross section for ^{235}U.

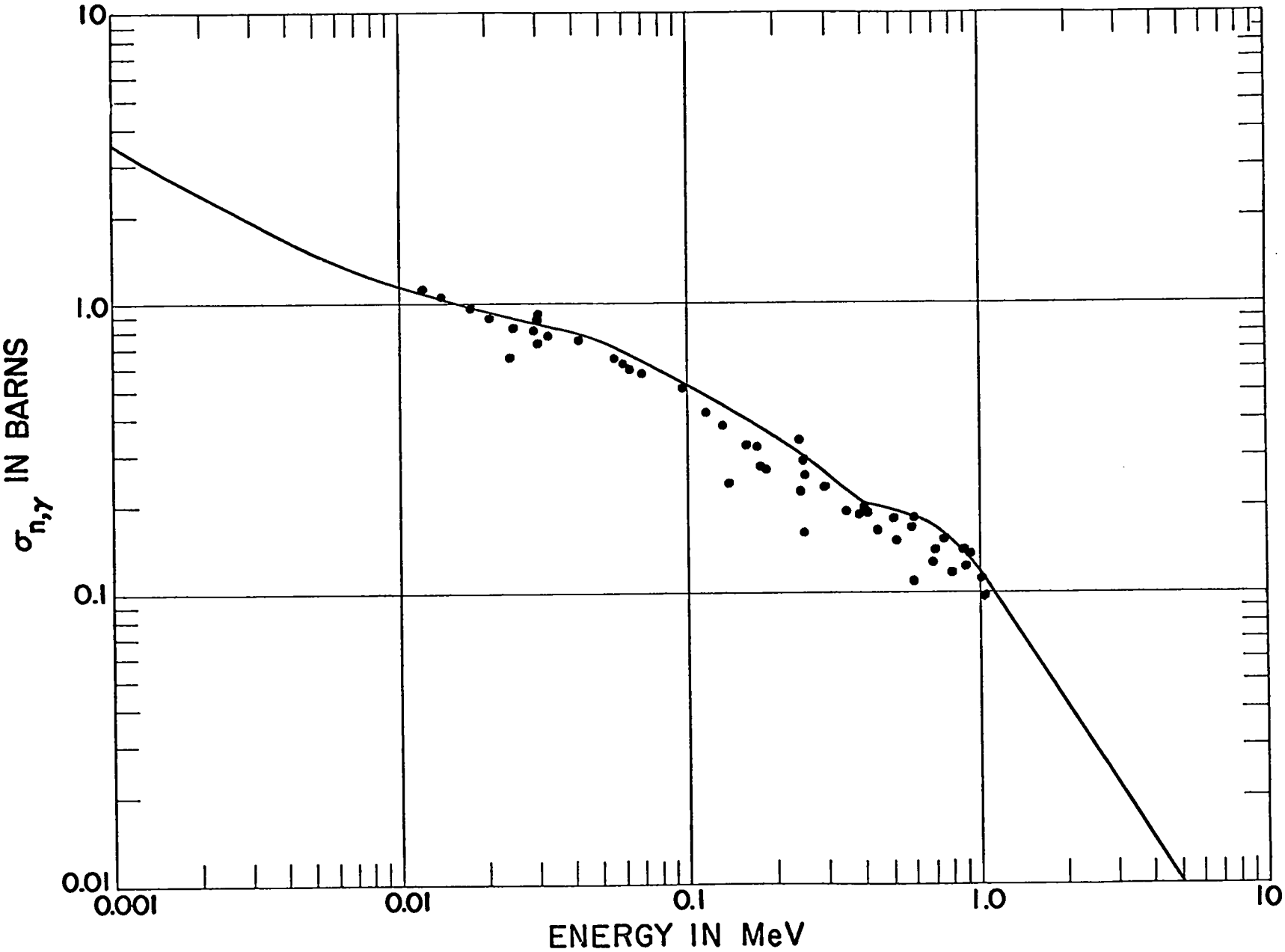

Fig. 2. Radiative capture cross section for ^{235}U.

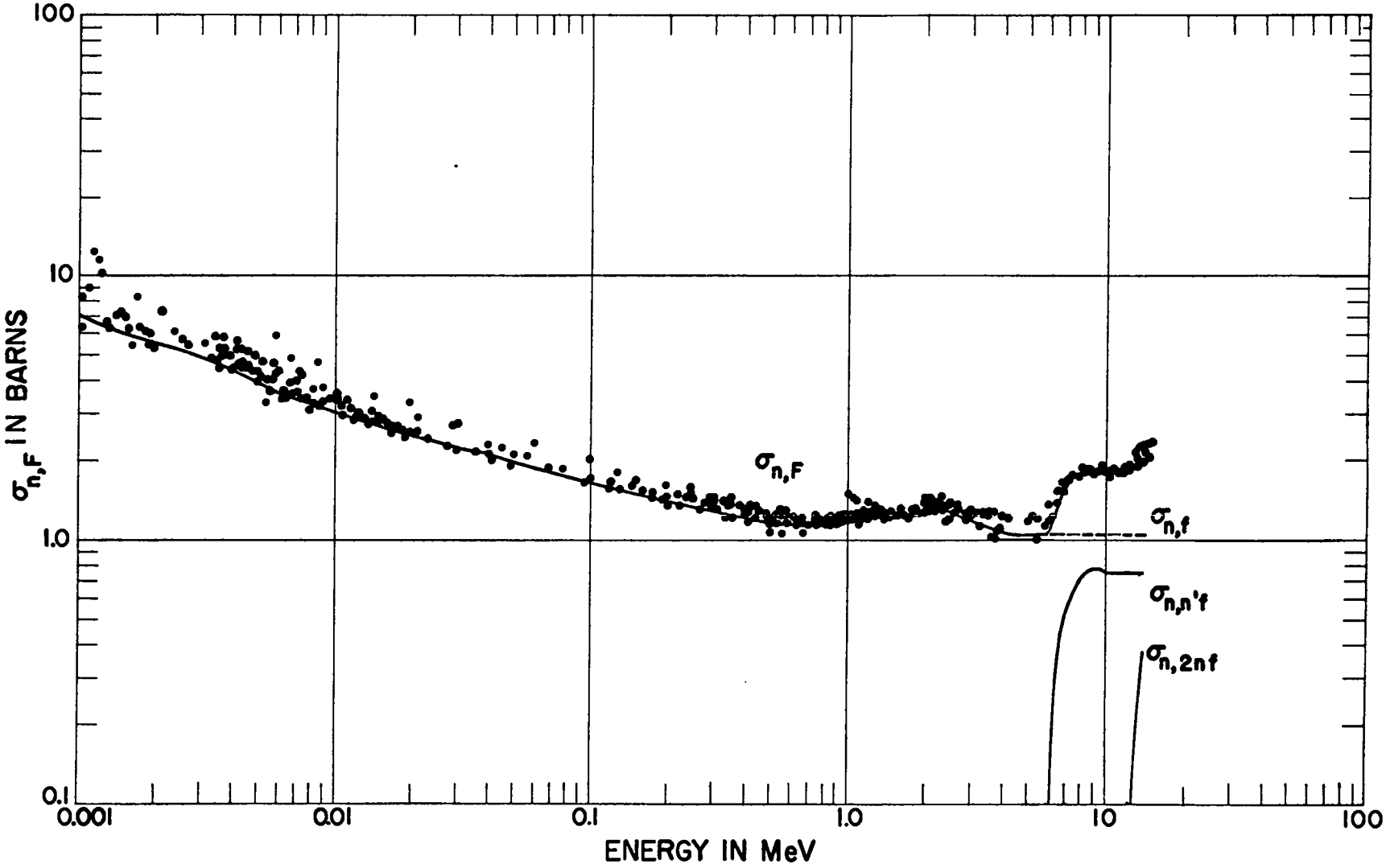

Fig. 3. Fission cross section for ^{235}U.

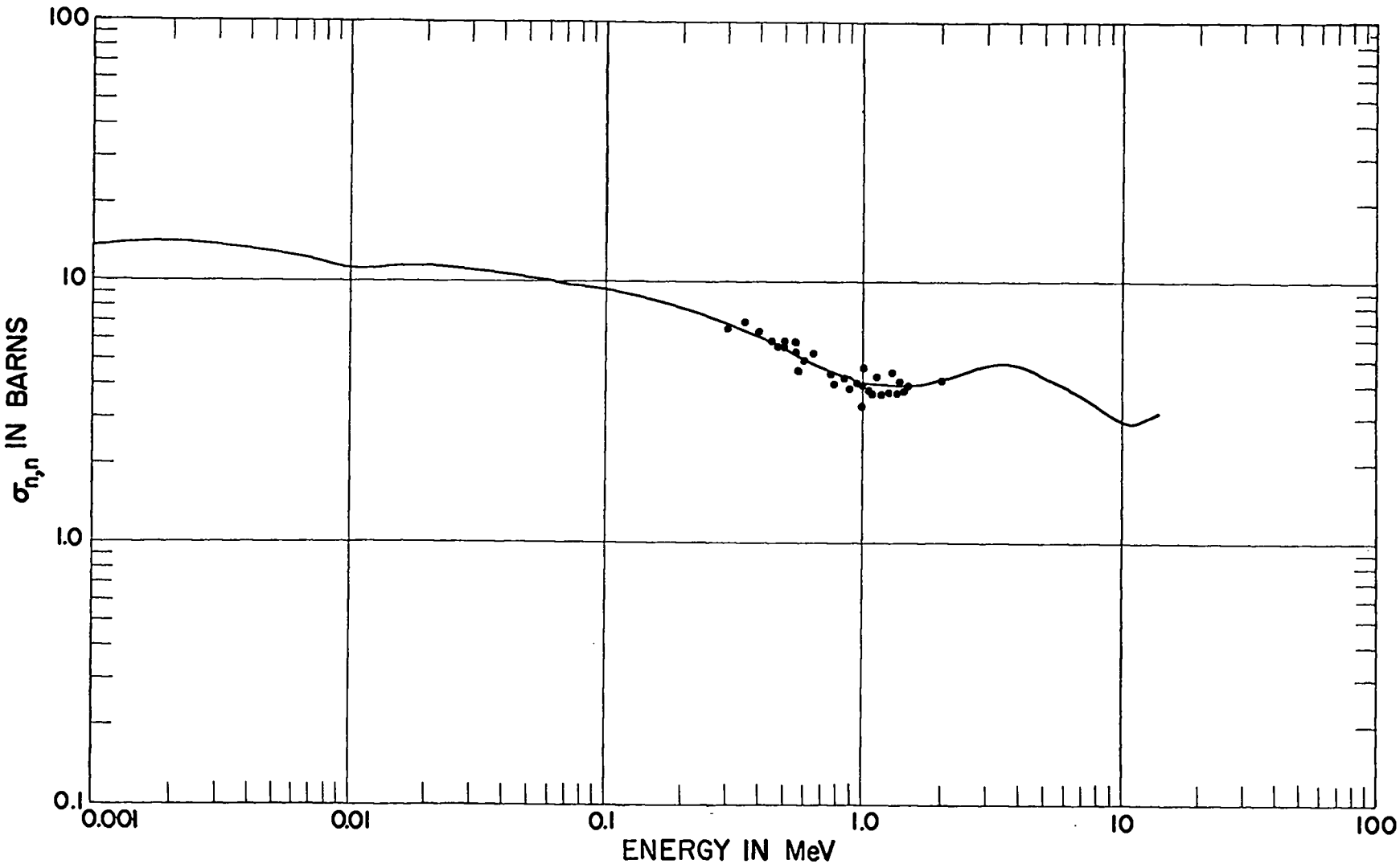

Fig. 4. Elastic scattering cross section for ^{235}U.

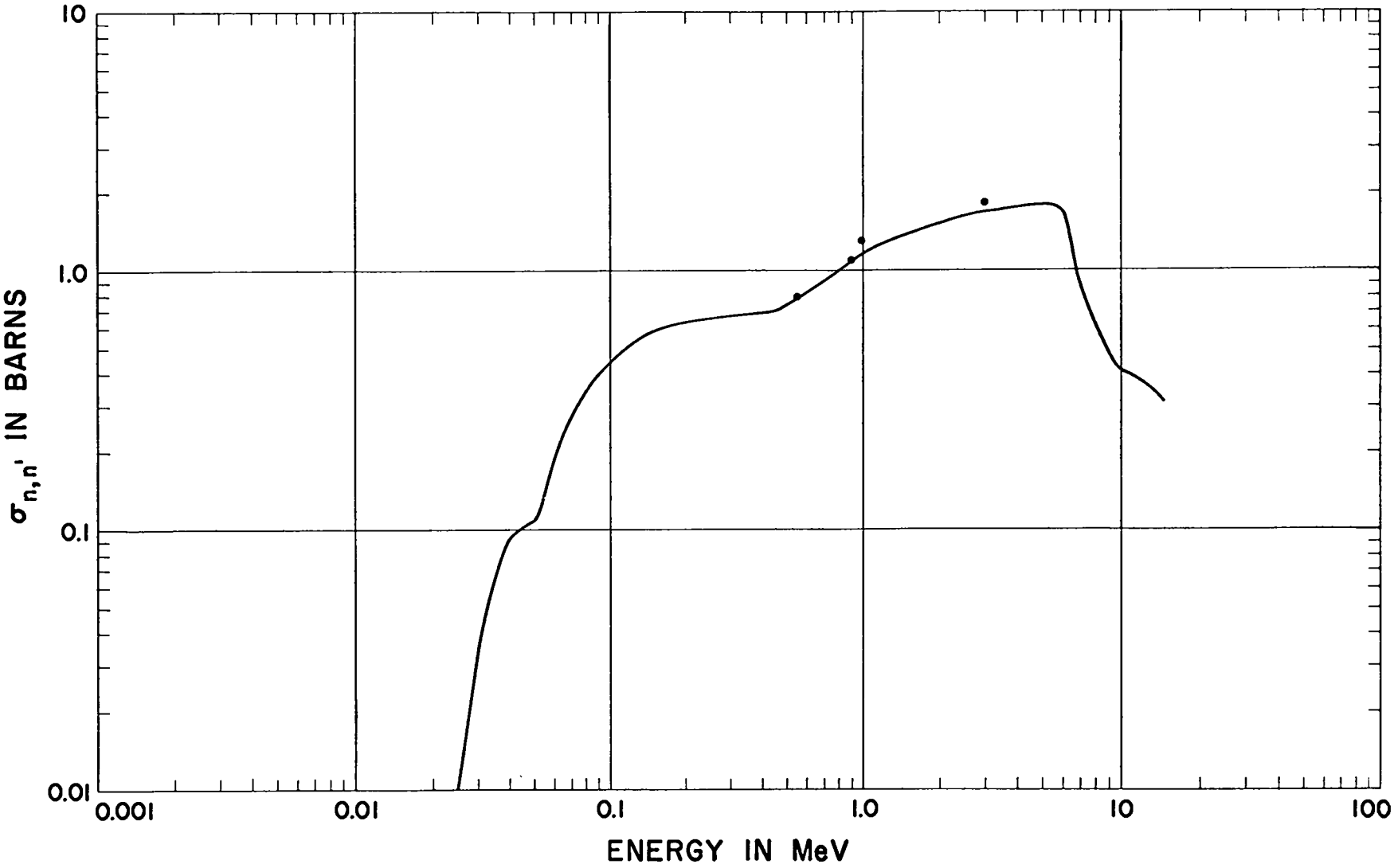

Fig. 5. Inelastic scattering cross section for ^{235}U.

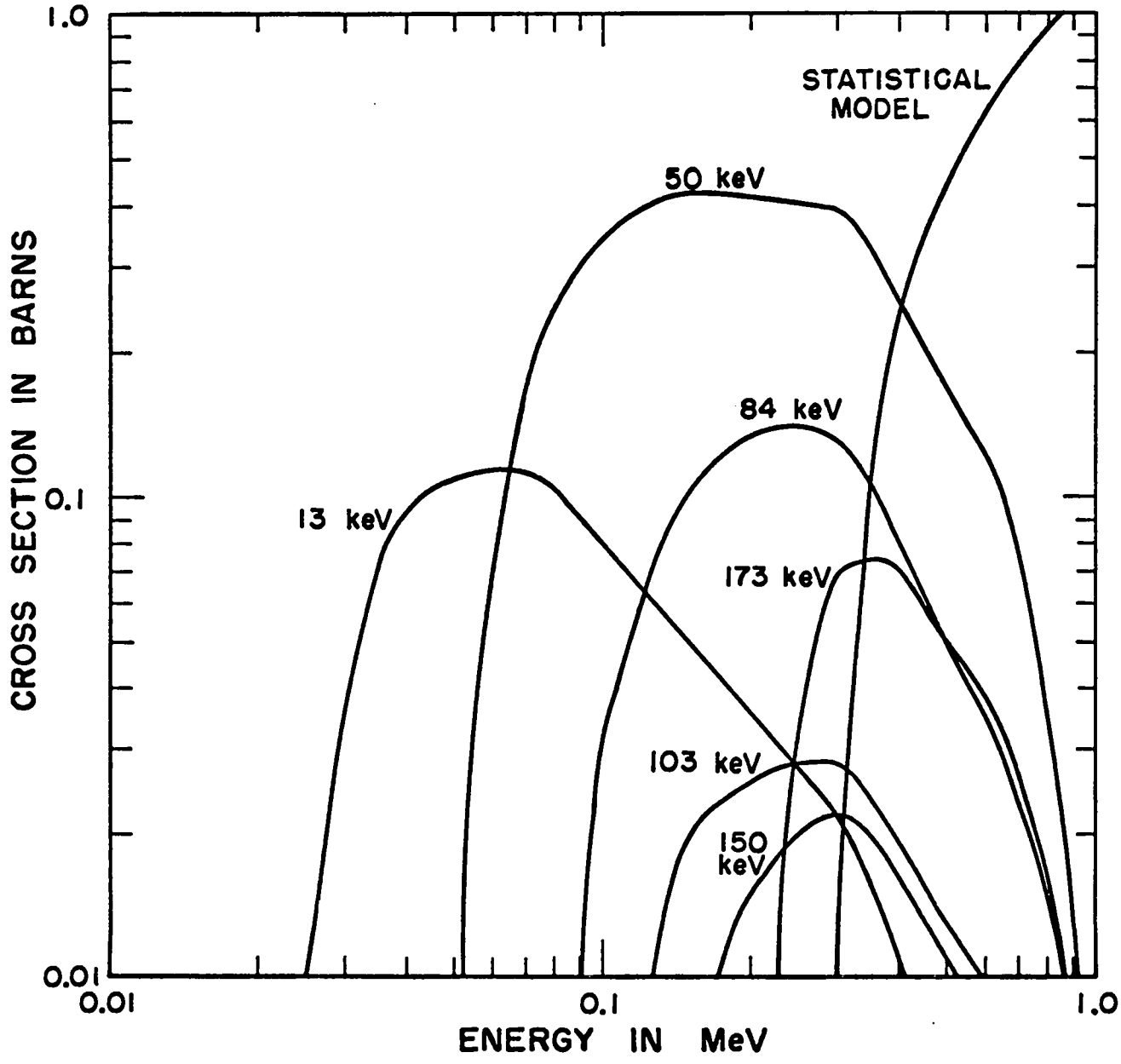

Fig. 6. Partial inelastic scattering cross sections for ^{235}U.

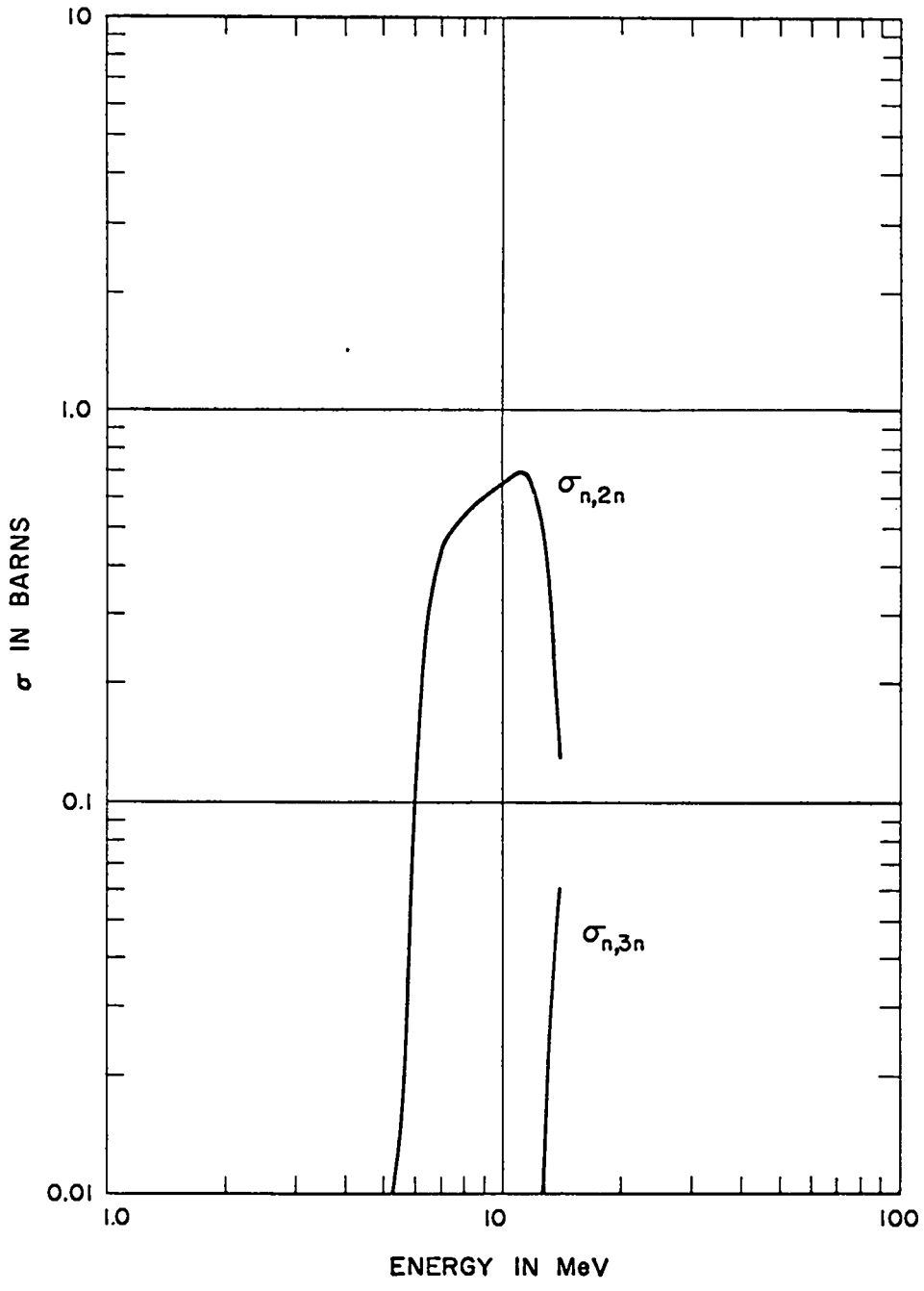

Fig. 7. $\sigma_{n,2n}$ and $\sigma_{n,3n}$ for ^{235}U.

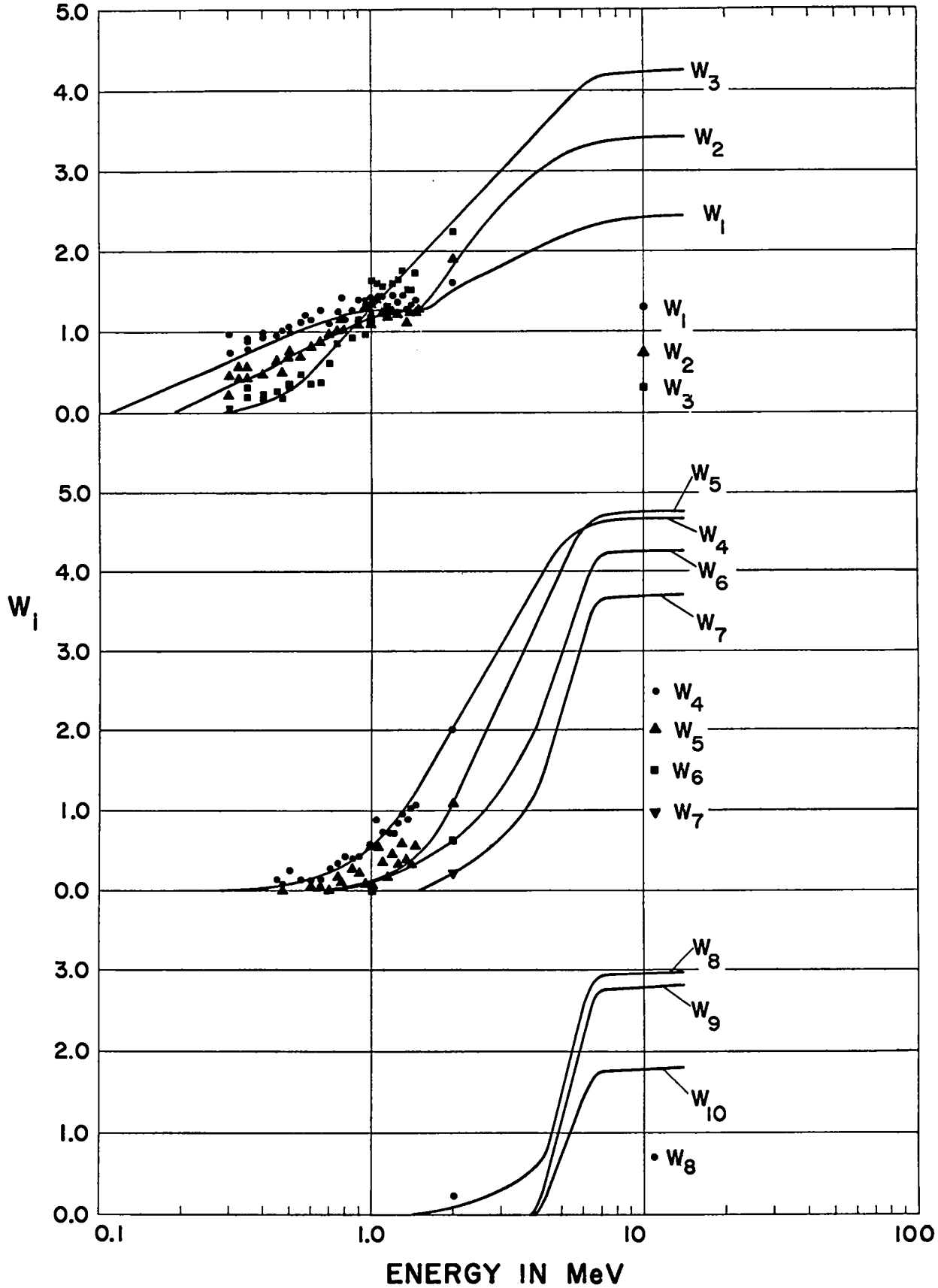

Fig. 8. Elastic scattering Legendre coefficients for ^{235}U.

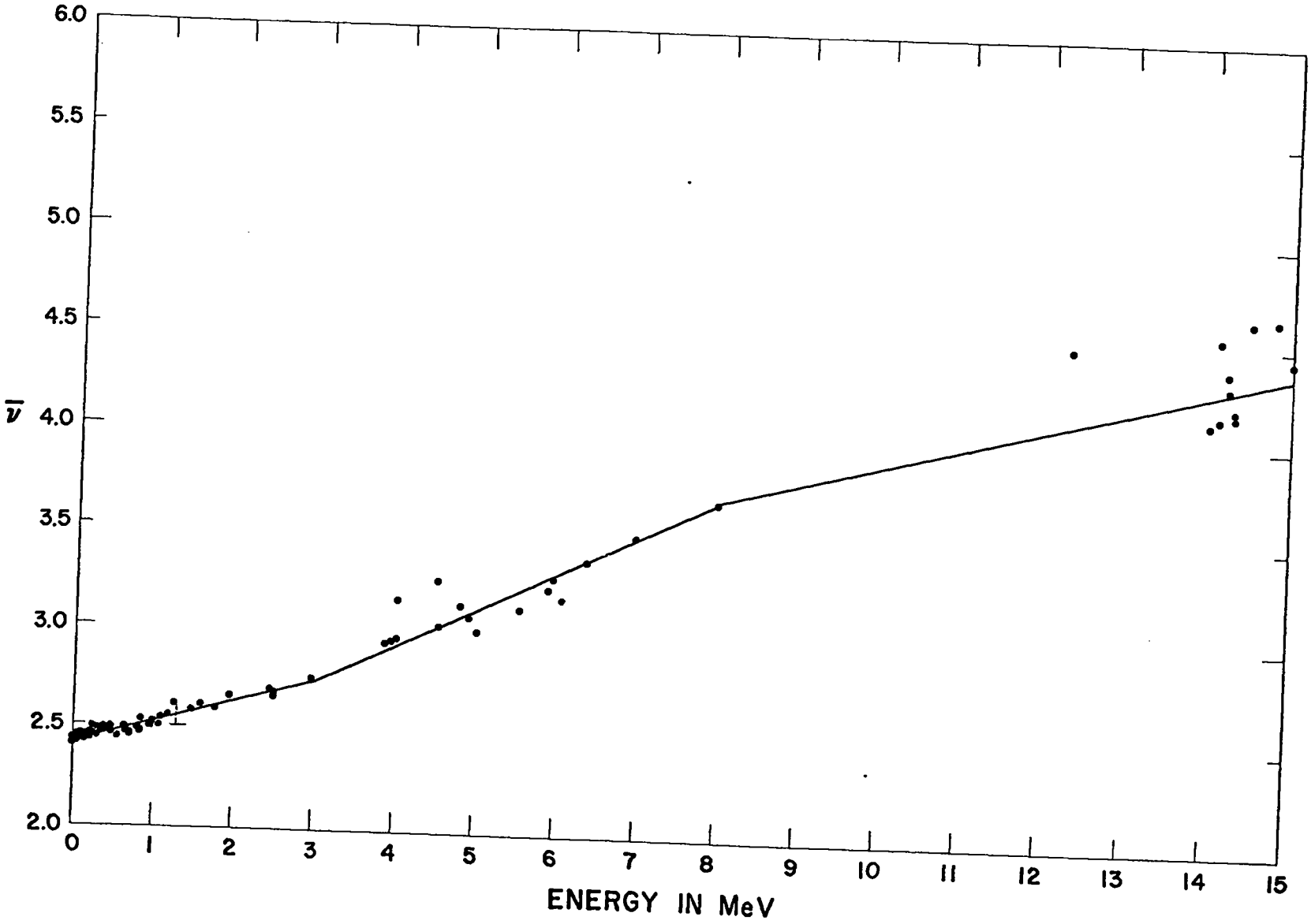

Fig. 9. Mean number of neutrons per fission for ^{235}U.

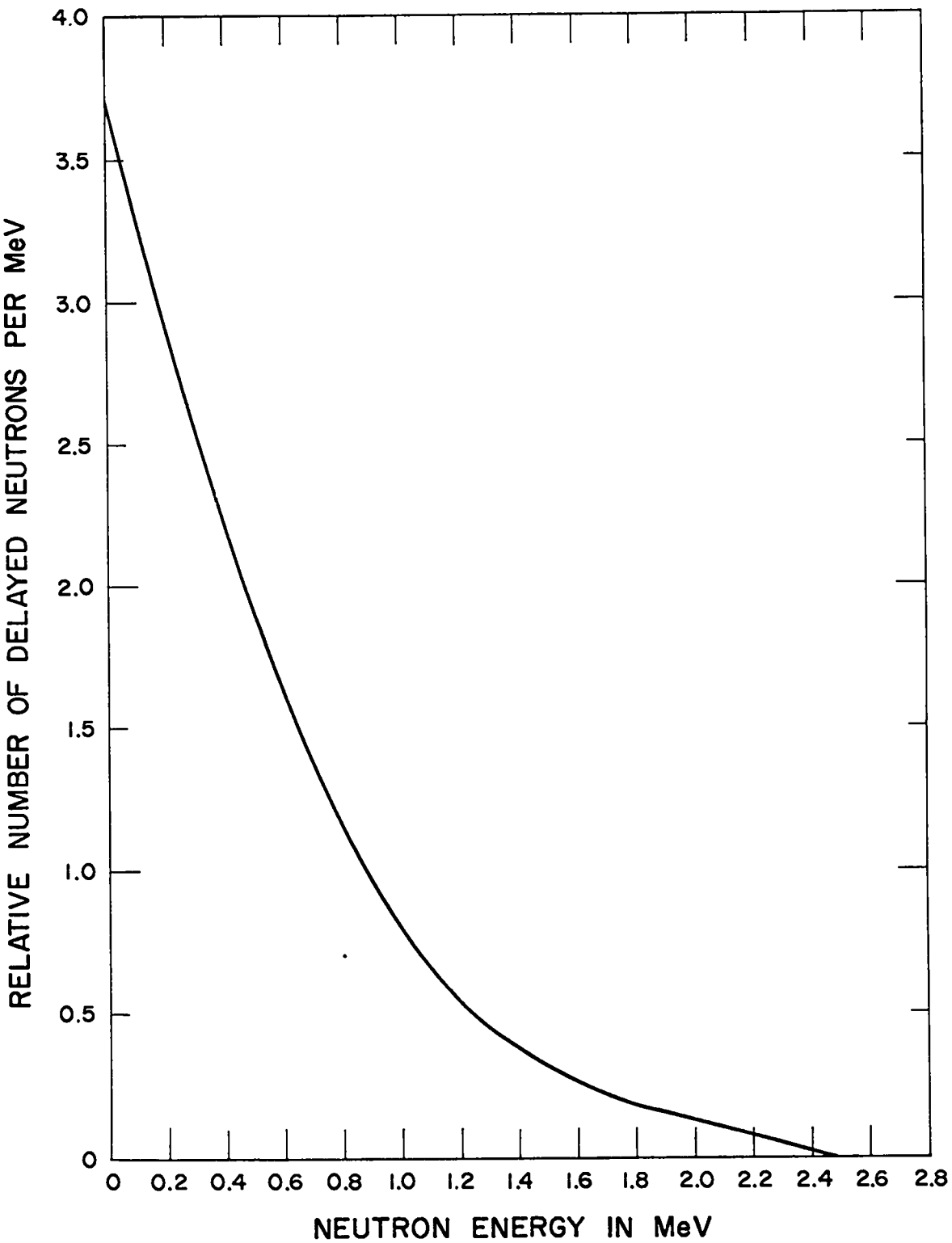

Fig. 10. Delayed neutron energy distribution for ^{235}U and ^{238}U.

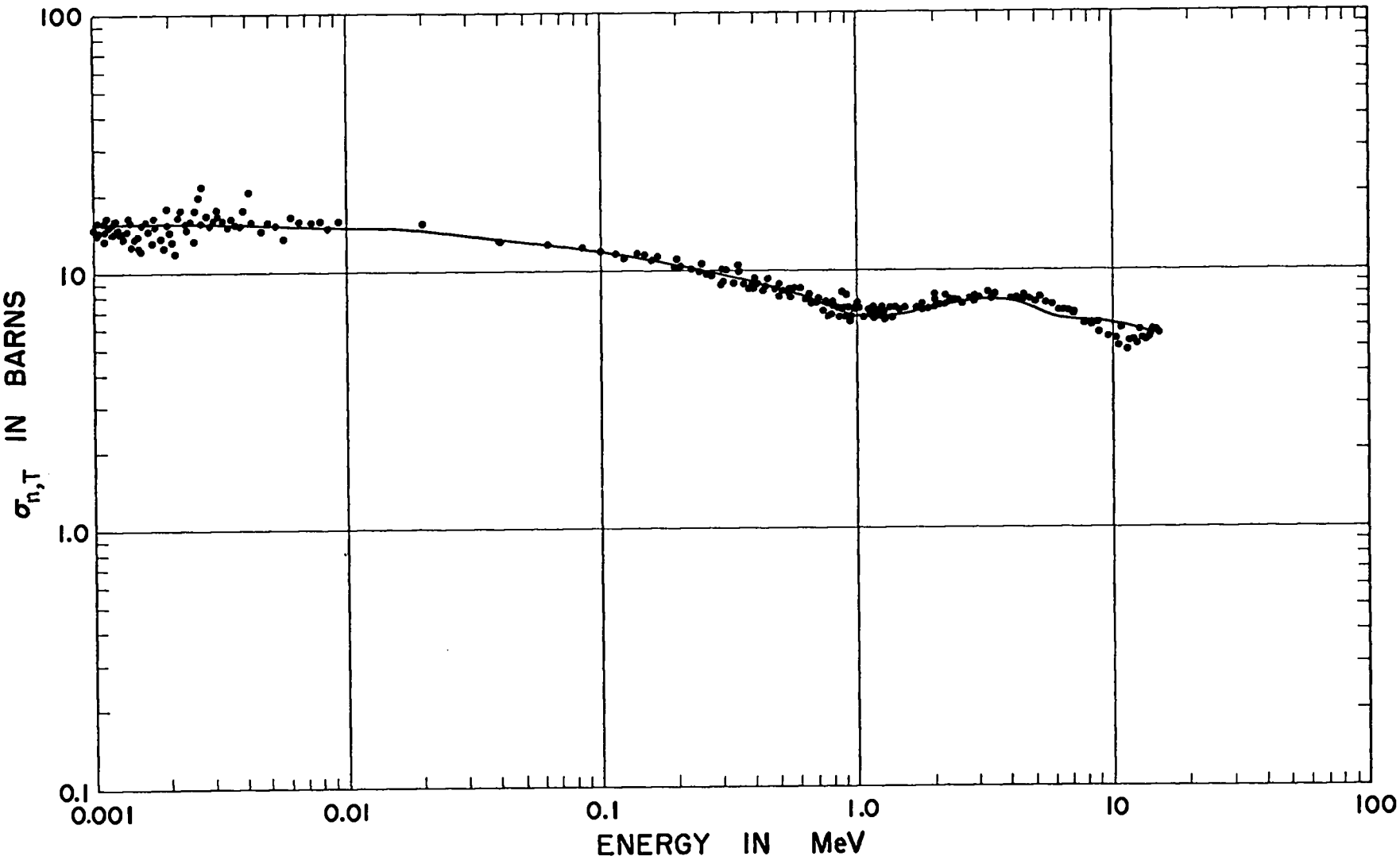

Fig. 11. Total cross section for ^{238}U.

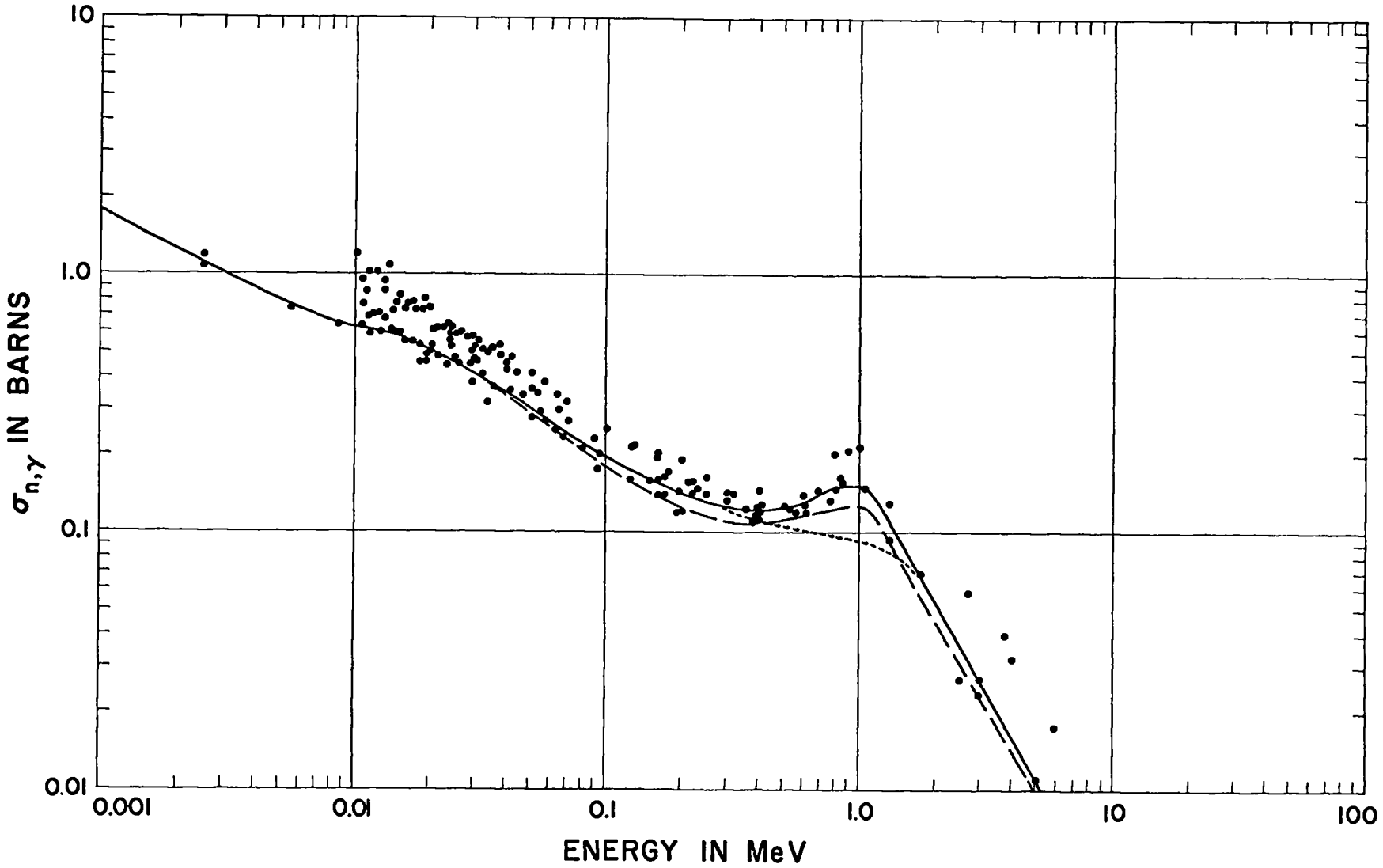

Fig. 12. Radiative capture cross section for ^{238}U. The solid curve is a "best fit" to the more recent data. The dotted curve, which is identical to the solid curve except between 0.3 and 1.8 MeV, is the recommended curve. Both the dotted and dashed curves are based on integral experiment comparisons.

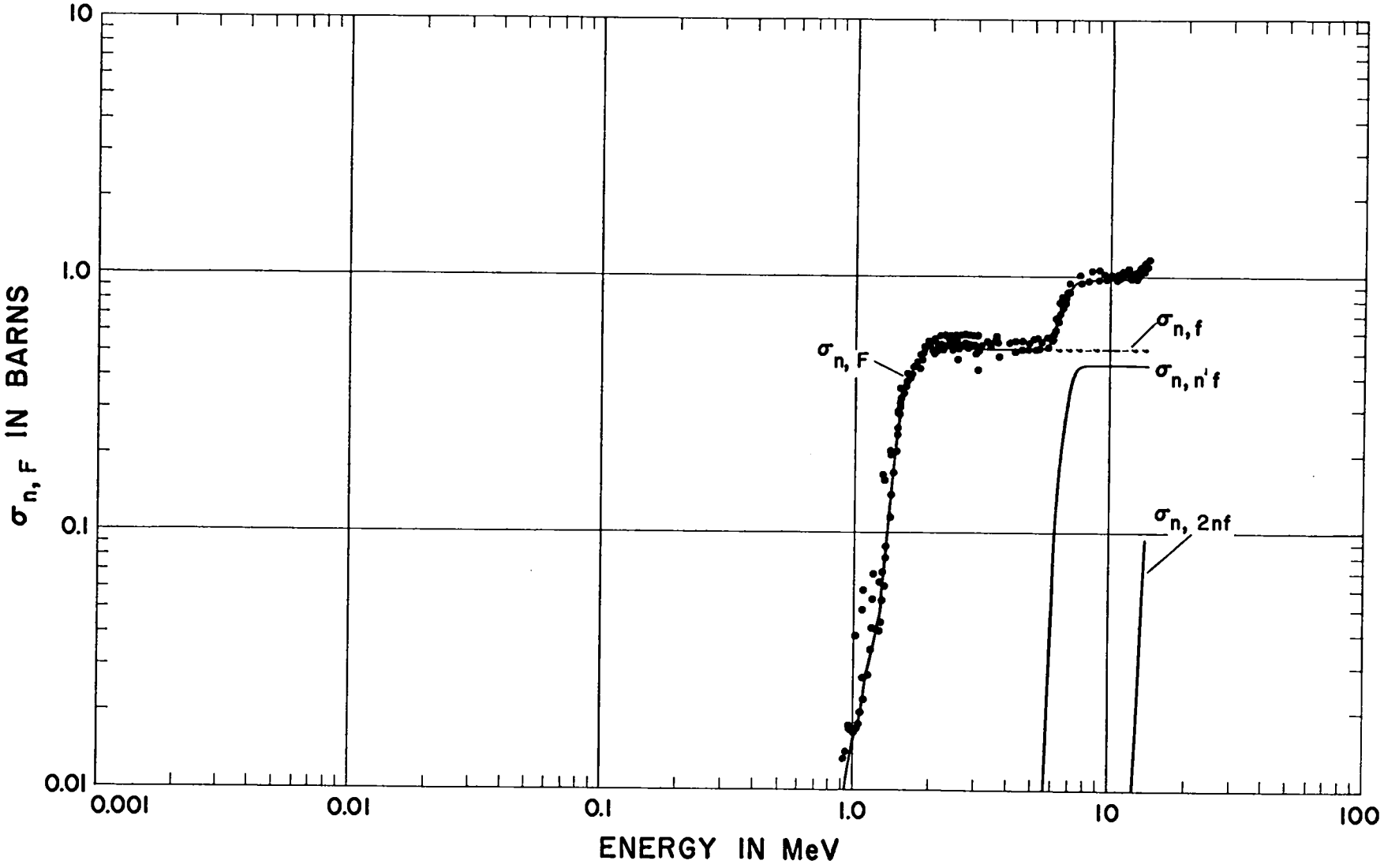

Fig. 13. Fission cross section for ^{238}U.

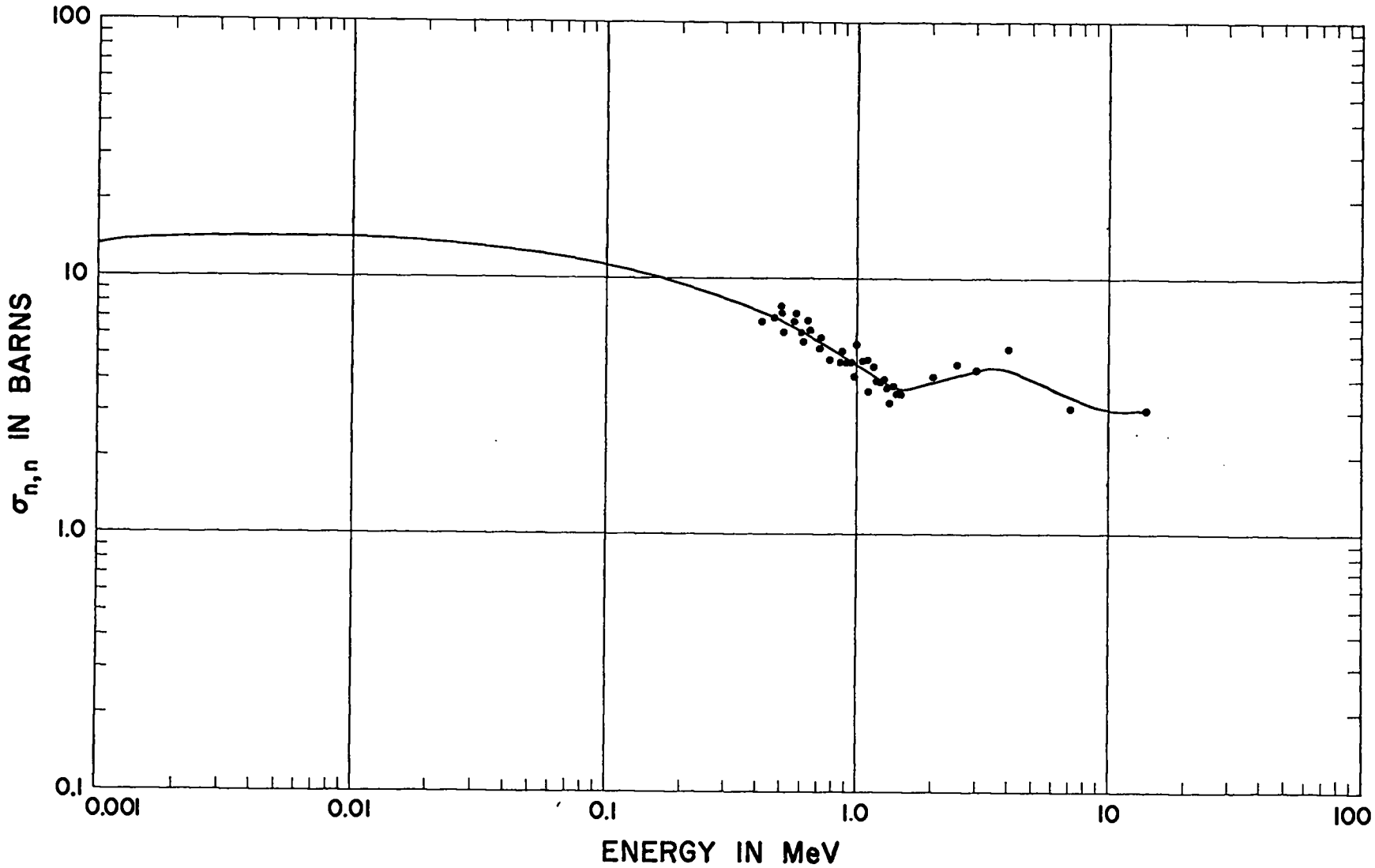

Fig. 14. Elastic scattering cross section for ^{238}U.

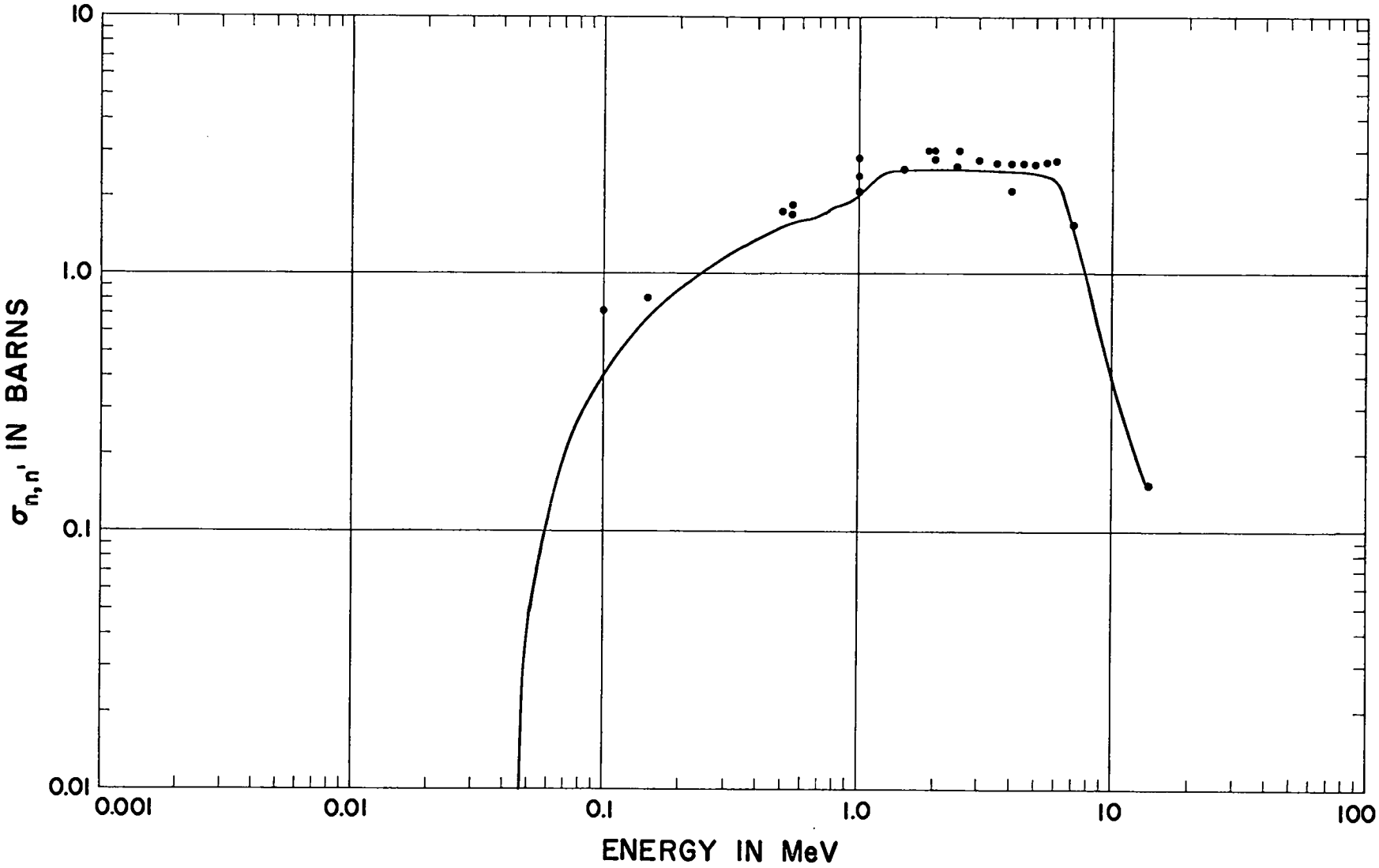

Fig. 15. Inelastic scattering cross section for ^{238}U.

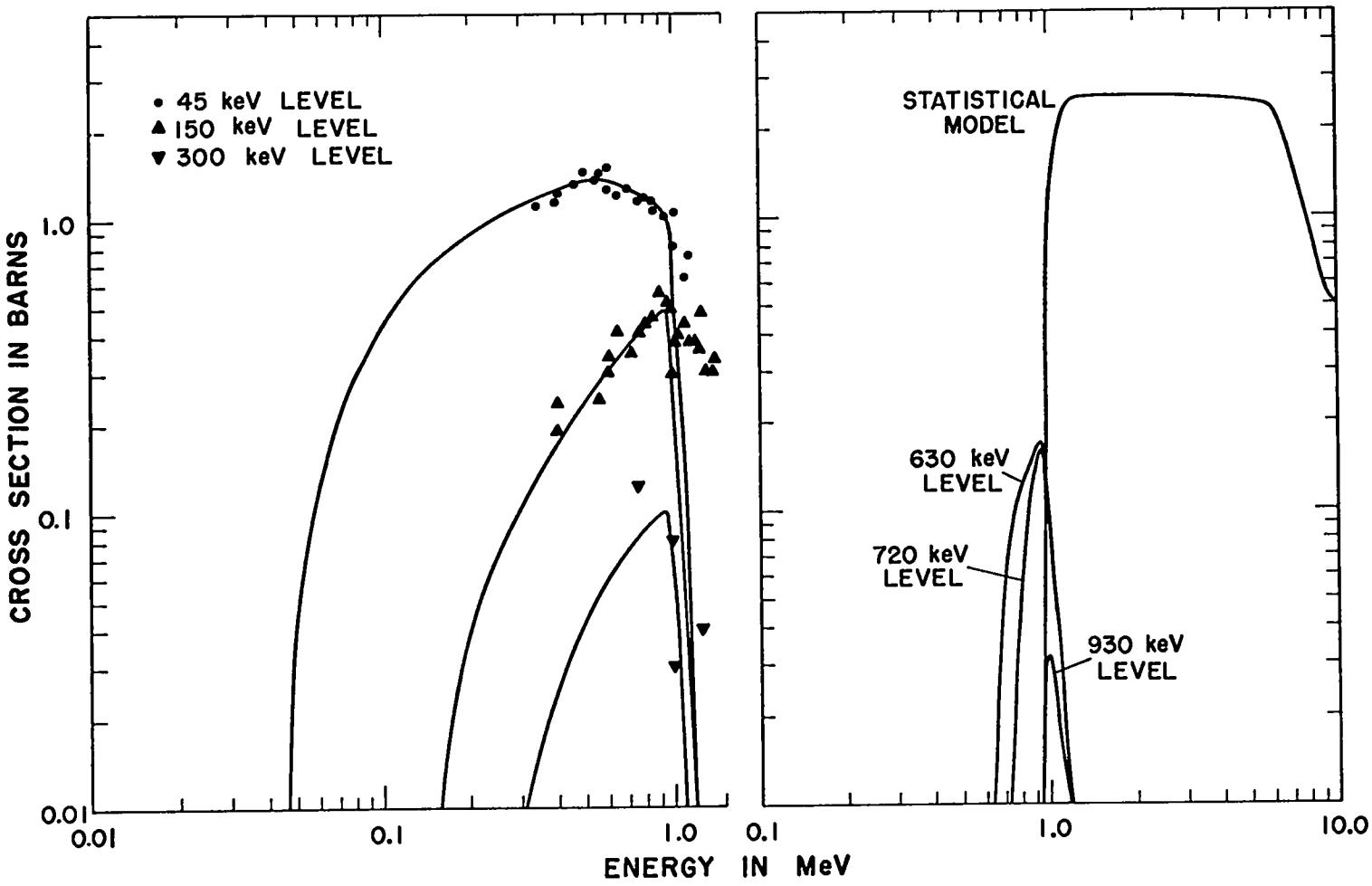

Fig. 16. Partial inelastic scattering cross sections for ^{238}U.

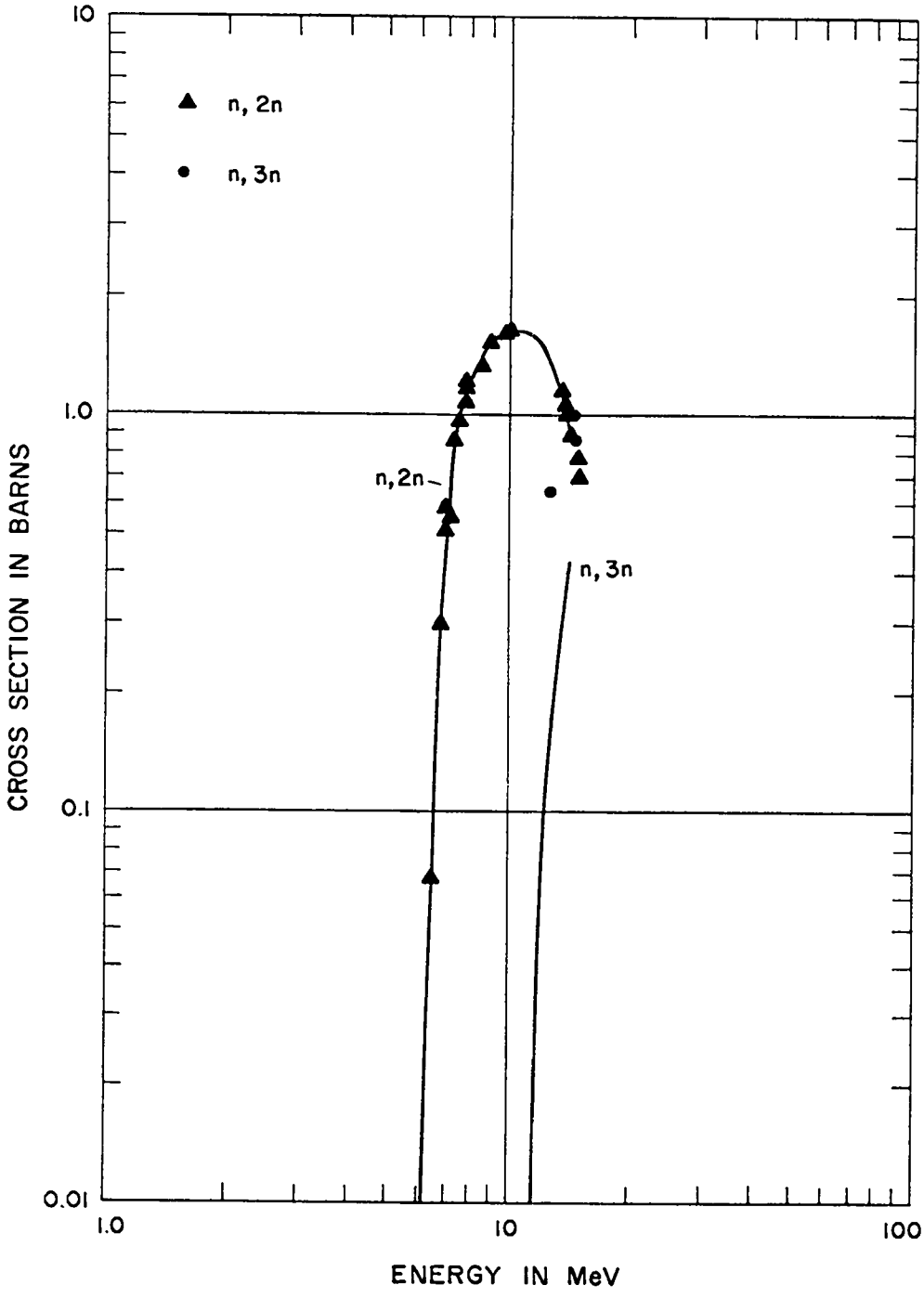

Fig. 17. $\sigma_{n,2n}$ and $\sigma_{n,3n}$ for ^{238}U.

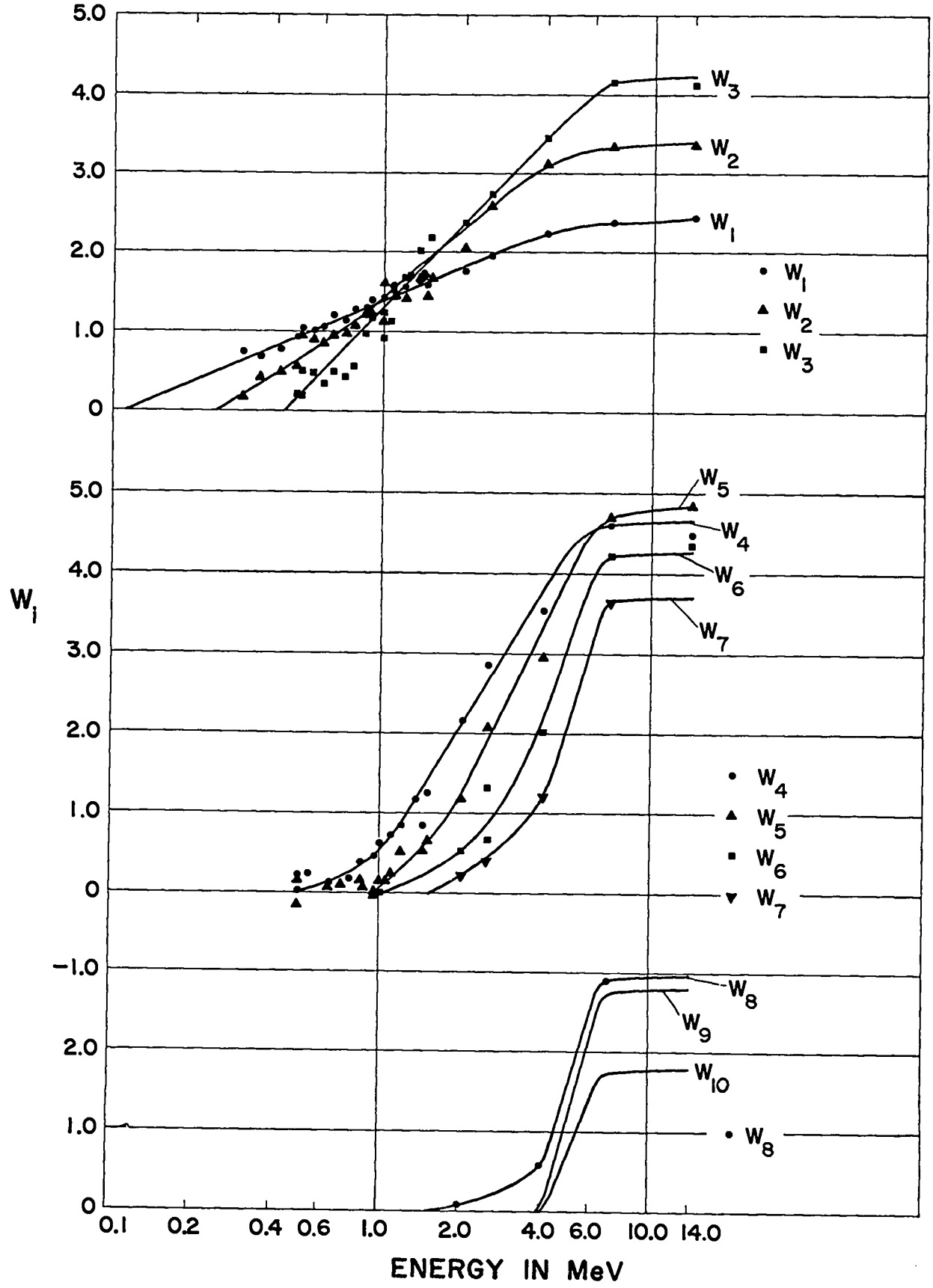

Fig. 18. Elastic scattering Legendre coefficients for ^{238}U.

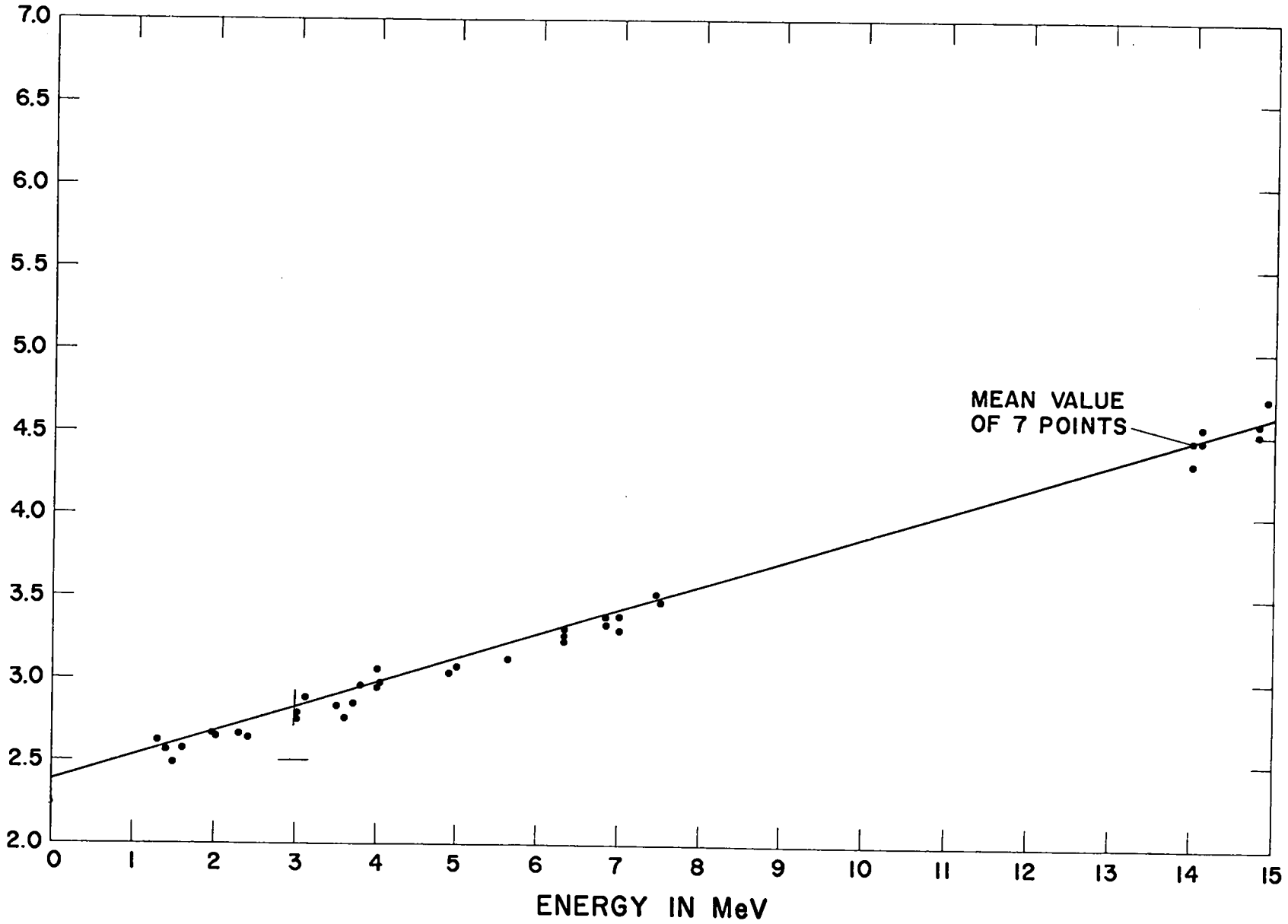

Fig. 19. Mean number of neutrons per fission for ^{238}U.